ResearchGate

See discussions, stats, and author profiles for this publication at: https://www.researchgate.net/publication/301770216

Bog iron ore as a resource for prehistoric iron production in Central Europe — A case study of theWidawa catchment area in eastern Silesia, Poland

Article *in* Catena · April 2016

DOI: 10.1016/j.catena.2016.04.002

CITATIONS
16

READS
789

4 authors, including:

Michael Thelemann
Senate Department for the Environment, Transport and Climate Protection
6 PUBLICATIONS **34** CITATIONS
SEE PROFILE

Wiebke Bebermeier
Freie Universität Berlin
39 PUBLICATIONS **261** CITATIONS
SEE PROFILE

Philipp Hoelzmann
Freie Universität Berlin
108 PUBLICATIONS **2,859** CITATIONS
SEE PROFILE

Some of the authors of this publication are also working on these related projects:

An Integrated Socio-EcoHydrological Framework to Assess and Evaluate Urban Water Security: A Geoinformatics based Water Security Assessment Approach for Kolkata city, India View project

Geoarchaeology in the surroundings of the Late Bronze Age "Royal Tomb" ("Königsgrab") of Seddin View project

All content following this page was uploaded by Philipp Hoelzmann on 31 August 2020.

The user has requested enhancement of the downloaded file.

Catena xxx (2016) xxx–xxx

Contents lists available at ScienceDirect

Catena

journal homepage: www.elsevier.com/locate/catena

Bog iron ore as a resource for prehistoric iron production in Central Europe — A case study of the Widawa catchment area in eastern Silesia, Poland

Michael Thelemann [a,c,*], Wiebke Bebermeier [a,c], Philipp Hoelzmann [a,c], Enrico Lehnhardt [b,c]

[a] Freie Universität Berlin, Institute of Geographical Sciences, Physical Geography, Malteserstraße 74-100, 12249 Berlin, Germany
[b] Freie Universität Berlin, Institute of Prehistoric Archaeology, Fabeckstraße 23-25, 14195 Berlin, Germany
[c] Excellence Cluster Topoi, Topoi Building Berlin-Dahlem, Hittorfstraße 18, 14195, Berlin, Germany

ARTICLE INFO

Article history:
Received 15 October 2015
Received in revised form 31 March 2016
Accepted 1 April 2016
Available online xxxx

Keywords:
Bog iron ore
Prehistoric iron smelting
Geochemical fingerprinting
Prehistoric iron slags
Portable ED-XRF
Przeworsk culture (6)

ABSTRACT

Spreading from the Near East in the declining Bronze Age from the 2nd millennium BCE onwards, the technique of iron smelting reached Eastern Silesia, Poland, in approximately the 2nd century BCE (pre-Roman Iron Age). At this time the region of the Widawa catchment area was inhabited by the Przeworsk culture. While the older moraine landscape of the study area lacks ores from geological rock formations, bog iron ores were relatively widespread and, due to their comparatively easy accessibility, were commonly exploited for early iron production. This paper investigates the mineralogical and elemental composition of local bog iron ore deposits and iron slag finds, as a by-product of the smelting process, also taking into account the state of the art in research regarding the formation, distribution and utilization of bog iron ores and considering data from comparative studies.

The crystalline mineralogical composition of local bog iron ores is dominated by quartz (SiO_2) and goethite (α-FeO(OH)), in contrast to slag samples in which fayalite (Fe_2SiO_4), wüstite (FeO) and quartz, with traces of goethite, represent the main minerals. Ores and slags are both characterized by notable hematite (Fe_2O_3), magnetite (Fe_3O_4) and maghemite (γ-Fe_2O_3) contents. Analyzed bog iron ore samples show iron contents of up to 64.9 mass% Fe_2O_3 (equivalent to 45.4 mass% Fe), whereas the iron contents of bloomery slags vary between 48.7 and 72.0 mass% FeO (equivalent to 37.9 and 56.0 mass% Fe). A principal component analysis of the element contents, which were quantified by portable energy-dispersive X-ray fluorescence spectrometry, indicates local variations in the elemental composition. The results of this study show that bog iron ores are relatively widely distributed with spatially varying iron contents along the Widawa floodplain but present-day formation conditions, such as changed groundwater levels, are negatively affected by modern land-use practices, such as agriculture and melioration measures.

© 2016 Elsevier B.V. All rights reserved.

1. Introduction

First iron smelting attempts date back to the 2nd millennium BCE in the Near East (Pleiner, 2000; Yalçin, 2000; Bebermeier et al., accepted). Over the following two millennia this technology was disseminated all over Europe and probably arrived in the study area of Eastern Silesia, Poland, in approximately the 2nd century BCE (Madera, 2002). In the pre-Roman Iron Age the region of the Widawa catchment area (Fig. 1) was inhabited by the Przeworsk culture (3rd century BCE to 5th century CE; Godłowski, 1985; Dąbrowska, 2003). Cultural and technological preconditions as well as requirements in terms of natural resources had to be met for the introduction of the innovative iron smelting. The main resources necessary for local iron production were wood for charcoal production, clay for the construction of bloomery furnaces, water for pre- and post-processing of ores and bloom and, above all, iron ores as a fundamental prerequisite (Koschke, 2002; Pleiner, 2000). For a local and independent iron production only places that united these resources were suitable for early iron smelting (Oberrascher, 1939). During the beginning of iron smelting a local small-scale production of iron was prevailing in the study area and the amounts of wood needed for the production of charcoal were rather negligible due to the occurrence of vast forested areas (Thelemann et al., in press).

While the glacially shaped older moraine landscapes of Northern and Central Europe mostly lack iron gangue minerals from geological rock formations, sedimentary bog iron ores were relatively widespread (Leb, 1983) and, due to its comparatively easy accessibility and reducibility, bog iron ore was commonly exploited for early iron production

* Corresponding author at: Freie Universität Berlin, Institute of Geographical Sciences, Physical Geography, Malteserstraße 74-100, 12249 Berlin, Germany.
E-mail address: michael.thelemann@fu-berlin.de (M. Thelemann).

http://dx.doi.org/10.1016/j.catena.2016.04.002
0341-8162/© 2016 Elsevier B.V. All rights reserved.

Please cite this article as: Thelemann, M., et al., Bog iron ore as a resource for prehistoric iron production in Central Europe — A case study of the Widawa catchment area in eastern ..., Catena (2016), http://dx.doi.org/10.1016/j.catena.2016.04.002

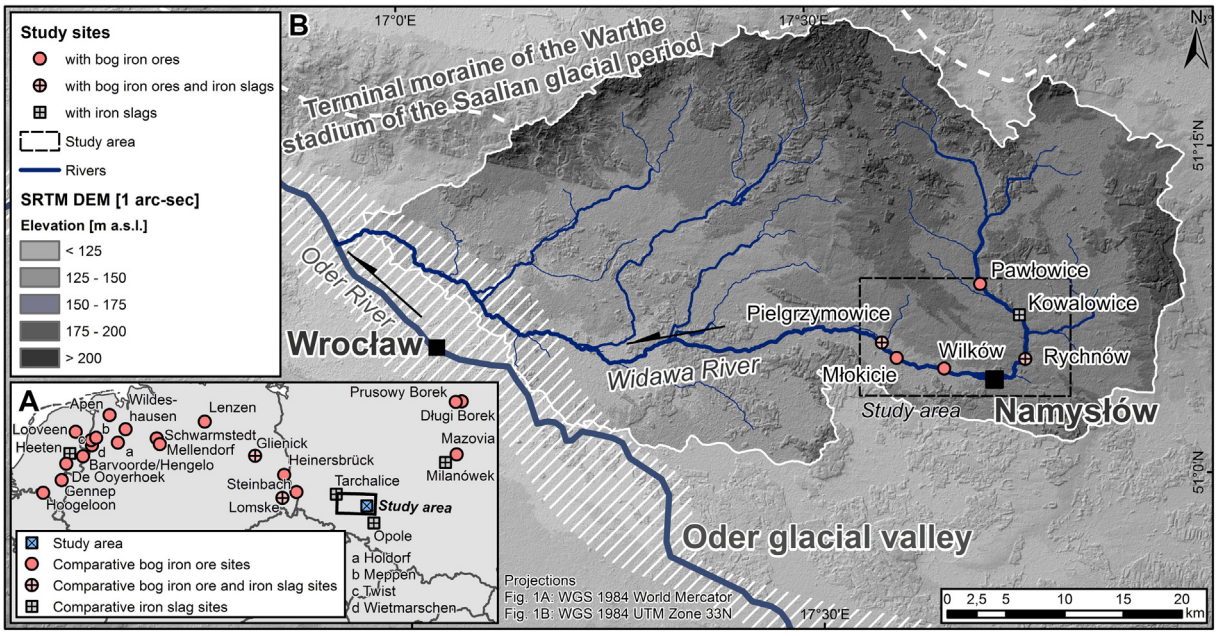

Fig. 1. Fig. 1 A. Location of the study area in Silesia and comparative case studies taken into account from literature on bog iron ores and iron slags; 1 B. Distribution of investigated bog iron ore deposits and iron slag findings in the catchment area of the Widawa River. Data sources: Fig. 1: A: Bog iron ores sites from Graupner (1982), Hensel (1986), Joosten et al. (1998), Ratajczak and Rzepa (2011), Puttkammer (2012), Brumlich et al. (2012); iron slag sites from Domanski (1972), Piaskowski (1976), Hensel (1986), Joosten et al. (1998), Puttkammer (2012), Brumlich et al. (2012), country borders Natural Earth Data; B: Digital elevation model from USGS (2000) SRTM-data; Widawa catchment area and rivers from KZGW (2015); terminal moraine and Oder glacial valley Liedtke (1981).

(Küster, 1999; Sperling, 2003; Leb, 1983; Brumlich et al., 2012; Sitschick et al., 2005).

This paper summarizes the state of the art of research on bog iron ores as a raw material for early iron smelting in Northern Central Europe. For the catchment area of the Widawa River geochemical and mineralogical data on local bog iron ores and slags are presented. As the chemistry of the bog iron ore – apart from other factors – dominates the chemical composition of the resulting slags, a focus is set on the analyses of the utilized ores.

The paper thus deals with the following research questions regarding the study area of the Widawa catchment area: (i) How can the present distribution and quality of bog iron ore resources be characterized, (ii) how is the mineralogical and elemental composition of iron slags and what conclusions can be drawn regarding the utilized ores and the early iron smelting techniques and (iii) how favorable was the study area for early iron production and are local variations in the quality of ores verifiable?

1.1. State of the art on bog iron ore

Bog iron ore is a subtype of bog ores. Main component of these ores is either iron or manganese. While manganese-rich bog ores are characterized by a gray-blackish color, the color of bog iron ores is brownreddish (Charlton et al., 2010; Krempler et al., 2004). It is assumed that based on the different colors early iron smelters were able to clearly distinguish between both types.

1.1.1. Morphology, elemental and mineralogical composition of bog iron ores

Bog iron ores are consolidated terrestrial accumulations dominated by iron minerals precipitated in sandy, silty or clayey sediments (Graupner, 1982; Sperling, 2003) with an iron content of >25 mass% Fe_2O_3 (Wünsche, 2007). In this study the term bog iron ore is used as an umbrella term for initial (<25 mass% Fe_2O_3) and developed (>25 mass% Fe_2O_3) bog iron ore samples in order to summarize the different bog iron ore characteristics and development stages.

Bog iron ores are distinguished into three different macromorphological types, which can be regarded as development stages: (i) a soft unstable form, (ii) randomly spread, nest-like distributed concretions, blocks or nodules and (iii) massive continuous horizons of horizontal, hard layers (Kaczorek and Sommer, 2003; Kaczorek et al., 2005; Landuydt, 1990; Sperling, 2003). Bog iron ore layers often reach a thickness of between several cm and >30 cm (Kaczorek et al., 2004). On the micro-scale the quartz-rich components of the parent sediment are separated from each other by an iron-rich matrix, which often dominates the structure of the ore (Krempler et al., 2004). The microstructure is represented by a relatively high capillarity and porosity and an often cellular fluctuating structure of micropores, which affects stability, weathering resistance and water absorbency (Krempler et al., 2004; Charlton et al., 2010; Lindbo et al., 2010). The stability and resistance depend on solidification and composition of the material and vary between crumbly, disintegrated and very solid fragments (Graupner, 1982; Krempler et al., 2004). Solidification mainly depends on the content of iron minerals and the degree of oxidization: the higher these are, the more cured the material (Graupner, 1982).

Table 1 shows a summary of the major oxide concentrations of bog iron ores based on a literature analysis. The elemental composition of bog iron ores is characterized by often considerable phosphorus and manganese contents of up to 8 mass% P_2O_5 and up to 10 mass% MnO (Wünsche, 2007; Landuydt, 1990; Sperling, 2003). The iron contents in bog iron ores mostly vary between 35 and 50 mass% Fe_2O_3 but can also reach up to 95 mass% Fe_2O_3 (Sitschick et al., 2005; Joosten et al., 1998; Sperling, 2003; Charlton et al., 2010). Silicon-dioxides (SiO_2), manganese-oxides (MnO), phosphorus-pentoxides (P_2O_5), calcium carbonates ($CaCO_3$) and oxides (CaO), nitrogen compounds and water also characterize the composition of bog iron ores (Krempler et al., 2004; Graupner, 1982; Puttkammer, 2012; Zwahr et al., 2000). Aluminium- (Al_2O_3), potassium- (K_2O), barium- (BaO), magnesium- (MgO), sodium-oxides (Na_2O), titanium-dioxides (TiO_2), total organic carbon (TOC) and total inorganic carbon (TIC) are also present in minor concentrations (Table 1; Krempler et al., 2004; Graupner, 1982; Puttkammer, 2012; Zwahr et al., 2000).

Please cite this article as: Thelemann, M., et al., Bog iron ore as a resource for prehistoric iron production in Central Europe — A case study of the Widawa catchment area in eastern ..., Catena (2016), http://dx.doi.org/10.1016/j.catena.2016.04.002

Please cite this article as: Thelemann, M., et al., Bog iron ore as a resource for prehistoric iron production in Central Europe — A case study of the Widawa catchment area in eastern ..., Catena (2016), http://dx.doi.org/10.1016/j.catena.2016.04.002

Table 1
Major oxide concentrations of bog iron ores from selected case studies in Poland, Germany and the Netherlands.

Source	Location		Sample	Fe_2O_3	FeO	Fe SUM	SiO_2	MnO	CaO	P_2O_5	Al_2O_3	K_2O	MgO	Na_2O	TiO_2
	Country	Site	ID	[mass%]	[mass%]	[mass%]	[mass%]	[mass%]	[mass%]	[mass%]	[mass%]	[mass%]	[mass%]	[mass%]	[mass%]
Graupner (1982)	Germany	Wietmarschen	E30	40.11	–	28.1[b]	49.59	0.17	0.14	0.41	0.71	0.24	0.02	0.10	0.03
		Twist	E33	49.18	–	34.4[b]	11.12	2.91	5.99	3.71	1.02	0.15	0.09	0.07	0.06
		Meppen	E34	68.10	–	47.6[b]	11.68	1.99	0.55	1.28	0.38	0.07	0.03	0.04	0.03
		Apen	E35	18.80	–	13.1[b]	62.89	2.50	1.01	1.55	3.09	0.80	0.20	0.38	0.16
		Holdorf	E36	41.80	–	29.2[b]	37.86	1.05	0.82	3.18	2.35	0.51	0.11	0.30	0.15
		Wildeshausen	E40	29.29	–	20.5[b]	44.88	0.85	1.56	3.26	3.88	0.91	0.23	0.50	0.31
		Mellendorf	E41	62.27	–	43.6[b]	17.20	0.56	0.63	3.33	1.22	0.26	0.09	0.15	0.08
		Schwarmstedt	E42	47.23	–	33.0[b]	31.00	0.63	0.41	3.65	2.08	0.60	0.11	0.26	0.15
		Lenzen	E50	41.18	–	28.8[b]	44.71	0.43	0.25	1.46	1.41	0.40	0.03	0.14	0.06
Hensel (1986)	Poland	Mazovia	R1	19.2	0.4	13.7[b]	58.2	5.40	0.8	1.11	2.4	–	0.1	–	0.17
			R2	23.0	0.7	16.6[b]	55.5	1.20	0.8	2.70	2.4	–	0.1	–	0.19
			R3	30.4	0.7	21.8[b]	24.0	13.5	2.2	3.78	3.4	–	0.3	–	0.15
			R4	14.2	0.5	10.3[b]	71.4	0.99	0.8	1.95	1.6	–	0.1	–	0.13
Joosten et al. (1998)	Netherlands	Heeten	A	46.9	10.3	40.8[b]	28.7	4.8	1.3	1.5	2.2	0.6	0.2	<0.1[a]	0.1
			B	72.5	np[a]	50.7[b]	20.0	2.7	<0.2[a]	1.7	1.8	0.4	<0.02[a]	0.2	0.1
		De Ooyerhoek	C	78.8	0.1	55.2[b]	14.1	0.8	0.8	3.6	0.9	0.2	0.2	<0.1[a]	0.1
			D	71.9	np[a]	50.3[b]	17.1	5.8	1.0	3.1	1.6	0.2	0.1	0.2	0.1
		Barvoorde	E	78.0	0.2	54.7[b]	16.1	0.6	<0.2[a]	3.1	1.4	0.3	<0.02[a]	<0.1[a]	0.1
		Hengelo	F	78.5	0.2	55.1[b]	10.9	6.1	1.1	1.0	1.4	0.3	<0.02[a]	<0.1[a]	0.03
		Looveen	G	72.2	0.2	50.7[b]	20.3	0.6	0.8	3.2	1.6	0.3	0.2	<0.1[a]	0.1
		Hoogeloon	H	94.8	0.4	66.6[b]	6.0	0.3	<0.2[a]	2.0	0.5	0.1	0.2	<0.1[a]	0.1
		Gennep	J	84.1	0.5	59.2[b]	13.9	0.3	0.3	2.2	1.4	0.1	0.1	<0.1[a]	0.1
Ratajczak and Rzepa (2011)	Poland	Długi Borek	I	35.07	–	24.5	21.36	0.23	3.27	8.39	1.90	0.29	0.22	0.13	0.12
		Prusowy Borek	I	50.45	–	35.3[b]	2.80	0.19	2.14	8.00	0.23	0.03	0.12	0.02	0.01
		Prusowy Borek	II	51.45	–	36.0[b]	7.72	0.18	2.67	2.37	0.41	0.08	0.08	0.04	0.02
Puttkammer (2012)	Germany	Steinbach	1	39.90	–	27.90	44.30	0.08	0.06	0.60	<BG[a]	0.58	<BG[a]	–	–
			2	34.80	–	24.34	52.60	0.08	0.06	0.49	<BG[a]	0.61	<BG[a]	–	–
			3	41.80	–	29.23	43.00	0.07	0.06	0.61	<BG[a]	0.58	<BG[a]	–	–
			4	37.60	–	26.29	49.90	0.07	0.06	0.51	<BG[a]	0.61	<BG[a]	–	–
		Lomske	1	41.00	–	28.67	30.20	0.49	0.34	2.26	<BG[a]	1.09	<BG[a]	–	–
			2	56.80	–	39.72	20.20	3.36	0.34	1.99	<BG[a]	0.74	<BG[a]	–	–
			3	34.50	–	24.12	32.01	1.74	0.84	2.21	<BG[a]	1.47	<BG[a]	–	–
			9A I	75.50	–	52.80	13.60	1.79	1.09	3.76	2.80	0.42	0.15	–	–
			9B II	88.20	–	61.70	7.90	0.35	0.37	0.73	1.57	0.21	0.06	–	–
Brumlich et al. (2012)	Germany	Glienick 14	EP 2/1	64.04	–	44.8b	13.47	1.35	1.15	4.06	1.04	0.09	0.11	0.05	0.04
			EP 2/2	69.86	–	48.9b	12.00	1.27	1.27	4.46	0.87	0.07	0.12	0.03	0.03
			EP 2/3	72.48	–	50.7b	10.03	1.12	1.14	4.19	0.48	0.03	0.08	<0.01a	0.02
			EP 2/4	62.27	–	43.6b	14.80	2.18	1.09	3.55	1.00	0.09	0.11	<0.01a	0.04

[a] Below respective detection limit.
[b] Converted from stated Fe_2O_3, FeO or Fe contents.

The composition of the ore largely depends on the elemental composition of the parent sediment in terms of geologic formations, the hydrological situation of the study area and the composition of groundwater fluxes (Kaczorek et al., 2005), which mainly function as a source of iron, manganese and phosphorus (Graupner, 1982). According to Kaczorek et al. (2005) heavy metal contents in bog iron ores, such as chrome (Cr), cobalt (Co), nickel (Ni), copper (Cu), zinc (Zn), cadmium (Cd) and lead (Pb), generally depend particularly on the parent sediment. The heavy metal contents of the Pleistocene parent sediments common in bog iron ores (Graupner, 1982; Oberrascher, 1939; Sitschick et al., 2005) are often relatively low (Kaczorek et al., 2005). Depending on the geogenic background considerable amounts of arsenic (As) are also typical in bog iron ores (Huisman et al., 1997; Banning et al., 2013).

The complex mineralogical composition of bog iron ores depends on the duration of stable physical-chemical conditions, the redox potential and the age of the iron minerals (Zwahr et al., 2000; Banning, 2008). Hardened bog iron ores are dominated by quartz components (SiO_2) and a limonite matrix (Zwahr et al., 2000; Krempler et al., 2004). Limonite is a generic term for a number of iron minerals, such as amorphous and crystalline iron-hydroxides and -oxides in varying compositions, mainly ferrihydrites ($Fe^{3+}{}_{10}O_{14}(OH)_2$) or yellow-brownish goethite (α-FeO(OH)) and reddish lepidocrocite ($Fe^{3+}O(OH)$) (Banning, 2008; Krempler et al., 2004; Kaczorek et al., 2004; Puttkammer, 2012; Wünsche, 2007; Zwahr et al., 2000). Variations in the mineral composition of the ferritic binding material influence morphology, color and stability, and also reflect the elemental composition of the ore (Krempler et al., 2004; Zwahr et al., 2000). The mineralogical composition of a bog iron ore layer can be divided into a ferric upper horizon with oxidizing conditions and a ferrous lower horizon with reducing conditions (Banning, 2008; Krempler et al., 2004; Landuydt, 1990; Leb, 1983). The top horizon tends to contain mineral phases such as hematites (Fe_2O_3), magnetites (Fe_3O_4) and maghemite (γ-Fe_2O_3) (Banning, 2008; Wünsche, 2007; Zwahr et al., 2000), whereas in the lower horizon it is rather siderites ($FeCO_3$), vivianites ($Fe_3^{2+}(PO_4)_2 \times 8H_2O$)) and pyrites ($FeS_2$) that prevail (Banning, 2008; Landuydt, 1990; Kaczorek et al., 2004; Arocena et al., 1990). This differentiation can be explained by the groundwater level (Graupner, 1982) and volatile small-scale changes in the redox potential during the bog iron ore formation (Landuydt, 1990). In the formation of siderites, vivianites and magnetites, also microorganisms play an important role since these minerals are products of bio-reduction by metal-reducing bacteria, produced as part of the geochemical cycle of iron in the biosphere (Banning, 2008; Shotyk, 1988). Illite ($(Al, Mg, Fe)_2(Si, Al)_4O_{10}[(OH)_2,(H_2O)]$), apatite ($Ca_5(PO_4)_3(F, Cl, OH)$, rutile ($TiO_2$), albite ($NaAlSi_3O_8$) and potash feldspar ($KAlSi_3O_8$) represent further typical minerals in bog iron ore deposits (Krempler et al., 2004).

1.1.2. Formation of bog iron ores

The basic requirement for the complex formation of bog iron ores is the presence of iron- and manganese-containing minerals and organic compounds in the catchment area, as is often the case in the context of Pleistocene deposits (Graupner, 1982; Oberrascher, 1939; Sperling, 2003). These minerals are destabilized through (bio)chemical weathering (Graupner, 1982) especially at pH values below 7 and a redox potential below 300 mV (Postawa and Hayes, 2013), often induced by humic or carbonic acids (Buurman and Jongmans, 2005). They then dissolve as ions or hydroxides into groundwater, interflow or capillary water and successively relocate (Graupner, 1982; Kaczorek et al., 2004; Leb, 1983; Sitschick et al., 2005; Zwahr et al., 2000). At locations close to the surface in an oxidizing or reducing milieu, particularly positively charged dissolved iron (Fe^{2+}) and manganese (Mn^{2+}) ions are precipitated or oxidized in the pore volume of a negatively charged parent sediment (Graupner, 1982; Kaczorek et al., 2004; Leb, 1983; Banning, 2008; Kaczorek et al., 2005; Sitschick et al., 2005; Sperling, 2003; Zwahr et al., 2000). During the bog iron ore formation the pore volume of the stationary parent sediment, mainly consisting of SiO_2 (Puttkammer, 2012), is gradually filled with a delivered matrix, which mainly consists of iron minerals (Oberrascher, 1939; Krempler et al., 2004). With further development of the ores the iron minerals develop to different Fe-phases: ferrihydrites ($Fe^{3+}{}_{10}O_{14}(OH)_2$) age to goethite and subsequently at a minimum temperature of 20 °C to hematite (Fe_2O_3), whereas lepidocrocite matures to maghemite (γ-Fe_2O_3) and subsequently also to hematite, depending on pH value, temperature and redox potential (Zwahr et al., 2000). With progressive development the amount of silicon in the ore decreases and the amount of iron increase. Pedogenetically – as part of a complex soil-geochemical process – the formation of bog iron ores is bound to gleys or gley podzols with higher varying redox potentials and a strong and constant perfusion of iron-containing water (Kaczorek et al., 2004; Graupner, 1982; Gall et al., 2003; Zwahr et al., 2000). Stable conditions in the zone of groundwater oscillation facilitate the repetitive contact of atmospheric oxygen with the groundwater and enable continuous, gradual bog iron ore formation (Oberrascher, 1939; Wünsche, 2007; Graupner, 1982; Sperling, 2003). The thickness, morphology and iron content of the developing ore layer depend on the duration and stability of favorable environmental conditions (Sperling, 2003), such as the groundwater level. Further factors influencing formation conditions are the iron-humus proportion, oxygen availability, groundwater flow velocity and climatic conditions (Graupner, 1982). Due to the complexity of the formation process, the shape, stability and quality of bog iron ore is highly variable on a small scale (Puttkammer, 2012; Krempler et al., 2004; Sperling, 2003; Kaczorek and Sommer, 2003).

1.1.3. Formation area

It is commonly accepted that bog iron ores are often bound to locations with a shallow groundwater table and hydromorphic structureless soils (Banning, 2008; Kaczorek and Sommer, 2003; Landuydt, 1990). There is widespread occurrence in the alluvial sandy, loamy to clayey soils of the glacially and fluvially shaped landscapes of the Central European flat lowlands, often in layers with high organic matter contents and/or plant activities (Kaczorek et al., 2005; Landuydt, 1990; Gall et al., 2003; Puttkammer, 2012; Salesch, 1996; Sperling, 2003). Areal bog iron ore deposits in particular are situated at the sandy margins of moist lowlands (Wünsche, 2007; Koschke, 2002; Küster, 1999; Oberrascher, 1939; Zwahr et al., 2000), whereas the nest-like distributed type is situated directly in wetter lowlands (Banning, 2008; Kaczorek and Sommer, 2003; Sperling, 2003; Salesch, 1996; Shotyk, 1988; Zwahr et al., 2000).

1.1.4. Formation phases and recent development

During the Holocene the main formation phases of bog iron ores are concentrated in warmer and wetter climate phases, particularly the late Boreal and the beginning of the Atlantic (Graupner, 1982; Wünsche, 2007; Sitschick et al., 2005). Empirical studies of growth rates of ores are lacking. According to estimations by Puttkammer (2012), the formation of bog iron ores may take between several hundred and a few thousand years depending on environmental conditions. According to Graupner (1982) considerable neoformations could not be detected in several case studies in Lower Saxony, Germany. Sitschick et al. (2005) assumes that neoformations are in principle possible also today, albeit restricted by centuries or millennia of agriculture, melioration measures and bog iron ore mining (Graupner, 1982; Leb, 1983; Puttkammer, 2012), which negatively influence some of the abovementioned prerequisites. Furthermore, recent changes in environmental conditions related to modern agriculture (e.g. drainage, deep ploughing) often not only inhibit bog iron ore formation but also cause the degradation of remaining depositions (Puttkammer, 2012).

1.1.5. The role of bog iron ores for early iron smelting with a focus on the Przeworsk culture

In order to produce iron from bog iron ores there is a variety of very different furnace types, such as slag-pit, slag-tapping or blast furnaces

Please cite this article as: Thelemann, M., et al., Bog iron ore as a resource for prehistoric iron production in Central Europe — A case study of the Widawa catchment area in eastern ..., Catena (2016), http://dx.doi.org/10.1016/j.catena.2016.04.002

Please cite this article as: Thelemann, M., et al., Bog iron ore as a resource for prehistoric iron production in Central Europe — A case study of the Widawa catchment area in eastern ..., Catena (2016), http://dx.doi.org/10.1016/j.catena.2016.04.002

Table 2
Major oxide concentrations of iron slags from selected case studies in Poland, Germany and the Netherlands.

Source	Location		Period	Sample	FeO	Fe_2O_3	Fe SUM	SiO_2	MnO	CaO	P_2O_5	Al_2O_3	K_2O	MgO	Na_2O	TiO_2	*RII*
	Country	Site		ID	[mass%]	[mass%]	[mass%]	[mass%]	[mass%]	[mass%]	[mass%]	[mass%]	[mass%]	[mass%]	[mass%]	[mass%]	
Domanski (1972)	Poland	Tarchalice	Roman period	I	62.98	0.36	50.21	28.22	0.38	0.23	3.12	2.02	–	0.39	–	–	1.04
				II	49.51	4.39	42.45	32.10	0.45	2.49	3.13	4.83	–	0.46	–	–	1.39
				III	61.96[b]	–	48.16	25.45	0.21	0.92	1.61	4.30	–	0.19	–	–	0.98
Piaskowski (1976)	Poland	Opole	2nd–5th cent. CE	N = n.a.	25.41–48.80	8.05–30.60	26.39–57.55	11.50–34.65	1.62–9.70	1.42–5.88	0.23–1.20	4.20–18.70	–	0.35–4.80	–	–	
					$\bar{x}$ 33.83	17.18	38.72	23.43	5.70	3.51	0.64	13.24	–	2.38	–	–	1.01
Hensel (1986)	Poland	Milanówek	Ancient period	I	35,5–51,6	13.5–35.3	44.7–54.0[b]	14.8–25.9	1.2–1.8	2.3–4.3	4.6–7.4	1.0–2.9	–	0.6–1.7	–	0.0–0.2	
					$\bar{x}$ 46.9	18.91	49.7[b]	19.7	1.59	3.3	6.0	1.6	–	1.0	–	0.1	0.72
				II	38.9–53.1	15.0–20.6	41.6–55.0[b]	16.9–30.1	2.0–3.0	2.2–4.0	2.7–5.2	1.4–3.2	–	0.1–1.3	–	0.1–0.2	
					$\bar{x}$ 47.6	17.4	49.2[b]	22.3	2.7	3.1	4.3	2.4	–	0.8	–	0.1	0.81
				III	30.0–55.0	12.7–31.10	43.1–56.7[b]	12.9–25.6	0.7–1.1	1.4–4.8	2.6–6.9	0.9–2.2	–	0.0–0.5	–	0.0–0.2	
					$\bar{x}$ 44.3	19.5	48.1[b]	20.0	1.0	3.3	5.4	1.6	–	0.2	–	0.1	0.76
Joosten et al. (1998)	Nether-lands	Heeten	2nd–5th cent. CE	He1A	58.4	2.8	47.4[b]	22.8	1.4	2.2	2.3	2.1	0.4	0.2	<0.1[a]	0.2	0.87
				He1B	52.8	2.3	42.7[b]	26.1	1.9	3.3	2.7	2.1	0.6	0.2	<0.1[a]	0.2	1.10
				He2A	62.8	2.8	50.8[b]	17.9	1.3	2.3	2.9	1.1	0.3	0.2	<0.1[a]	0.1	0.64
				He3A	62.1	4.2	51.2[b]	17.6	1.4	2.3	3.0	1.2	0.3	0.2	<0.1[a]	0.1	0.63
				He4A	64.0	2.0	51.2[b]	17.2	1.4	2.3	3.0	1.1	0.3	0.2	<0.1[a]	0.1	0.61
				HeG	56.1	13.1	52.8[b]	15.0	0.7	3.0	2.3	2.0	<0.04[a]	0.3	<0.1[a]	0.1	0.52
Puttkammer (2012)	Germany	Lomske	4th cent. CE	3/11	49.08[b]	–	38.15	32.53	3.93	1.66	1.78	3.43	0.97	0.20	0.16	0.27	1.47
				8/18	59.62[b]	–	46.34	25.39	0.45	1.56	1.69	3.14	0.69	0.21	0.13	0.20	1.01
Brumlich et al. (2012)	Germany	Glienick	8th cent. BCE–1st cent. CE	SP 1/1	62.70	9.98	55.72[b]	14.44	2.43	1.95	2.98	0.51	0.20	<0.05[a]	0.07	0.05	0.47
				SP 1/2	63.40	8.07	54.93[b]	13.33	2.58	1.95	3.08	0.31	0.15	<0.05[a]	0.05	0.03	0.43
				SP 2/1	58.90	5.87	49.89[b]	19.36	3.08	2.36	2.64	1.09	0.21	<0.05[a]	0.09	0.07	0.69
				SP 2/2	58.40	4.68	48.67[b]	19.85	2.72	2.07	2.56	1.30	0.21	<0.05[a]	0.10	0.08	0.73
				SP 3/1	53.90	4.15	44.80[b]	21.33	4.18	3.45	2.96	0.75	0.86	<0.05[a]	0.11	0.05	0.82
				SP 3/2	56.00	3.41	45.91[b]	21.69	3.84	3.13	2.86	0.93	0.63	<0.05[a]	0.13	0.05	0.82
				SP 6/1	56.99	8.69	50.38[b]	25.39	1.72	2.89	2.40	1.02	0.36	0.20	0.02	0.04	0.91
				SP 6/2	58.10	7.73	50.57[b]	25.05	1.69	2.89	2.43	1.05	0.35	0.19	0.02	0.04	0.90
				SP 7/1	58.59	8.87	51.75[b]	19.67	3.17	3.06	4.32	0.71	0.33	0.19	<0.01[a]	0.03	0.67
				SP 7/2	56.93	8.84	50.43[b]	20.75	3.22	3.28	4.61	0.77	0.36	0.18	0.01	0.03	0.73
				SP 8/1	63.48	7.63	54.68[b]	17.83	2.38	3.08	3.96	0.66	0.17	0.19	<0.01[a]	0.03	0.59
				SP 8/2	62.63	8.14	54.38[b]	18.15	2.39	3.10	3.98	0.64	0.17	0.20	<0.01[a]	0.03	0.60
				SP 9/1	55.13	10.71	50.34[b]	21.07	2.26	3.71	5.08	0.82	0.15	0.21	<0.01[a]	0.04	0.75
				SP 9/2	56.33	8.99	50.07[b]	21.66	2.31	3.78	5.14	0.80	0.16	0.20	<0.01[a]	0.04	0.78

[a] Below respective detection limit.
[b] Converted from stated Fe_2O_3, FeO or Fe contents.
[c] Reducible Iron Index (according to Charlton et al., 2010).

(Joosten et al., 1998), which strongly influence the morphology and microstructure of the resulting slags (Paynter, 2006; Joosten et al., 1998). For early iron smelting attempts in Eastern Silesia the technology of bloomery shaft furnaces with a slag pit was "almost solely" (Orzechowski, 2011) used by the Przeworsk culture (Orzechowski, 2007; Woźniak, 1978; Thelemann et al., in press). For this technique washed, roasted and crushed bog iron ores and charcoal are placed together in a clay furnace (Koschke, 2002). The base of the furnace is situated below the subsurface and consists of a pit where the slag solidifies (Woźniak, 1978). Possibly also further fluxing agents, such as limestone ($CaCO_3$) or basalt (containing manganese), are added to facilitate the smelting process in terms of lower process temperatures and to benefit the transition into the slag phase as it is described for Lusatia (Puttkammer, 2012; Koschke, 2002). Through additional air supply the necessary process temperatures of between 1100 and 1400 °C are reached (Graupner, 1982; Koschke, 2002). During the smelting process the iron in the ore is reduced to a spongy iron bloom (iron phase), which stays in the upper part of the furnace, while most of the other elements stream downwards as slag (slag phase) liquefied during the smelting (Graupner, 1982; Joosten et al., 1998; Koschke, 2002; Sperling, 2003, Puttkammer, 2012). During this process the iron (III) oxides of the ore (Fe_2O_3) are first reduced to magnetite (Fe_3O_4), then to wüstite (FeO) and finally to pure iron (Fe) (Schöner et al. 2003, Garner, 2011). In case of iron rich ores it is suggested that silicon-dioxide from technical ceramic, such as furnace wall or tuyeres, can react with the smelt (Veldhuijzen and Rehren, 2007), influencing the acidity and viscosity of the iron slag (Puttkammer, 2012). The produced slag melt represents the main by-product from iron smelting with a bloomery furnace (Puttkammer, 2012; Sperling, 2003). Due to reducing conditions during the smelting process the iron in the slag is primarily bound in FeO and not in Fe_2O_3 (Joosten et al., 1998; Puttkammer, 2012; Sperling, 2003). Table 2 shows a summary of the major oxide concentrations of iron slags based on the literature analysis. Since iron slags were separated from the bloom, they are usually characterized by lower iron and higher silicon contents than the originating bog iron ores (Graupner, 1982; Koschke, 2002; Puttkammer, 2012; Sperling, 2003).

Smelting with a bloomery furnace often results in between 10 and 20 mass% Fe being reduced to iron bloom, while the rest of the iron is transferred into the iron slag (Puttkammer, 2012; Sperling, 2003). The main factors for the success of the smelting process are the height and control of process temperatures, the quality of the ores and the viscosity of the iron slag (Puttkammer, 2012). The beginning of iron mining and smelting in the study area was probably limited to local production scales, as it is typical for Central Europe (Küster, 1999; Schwab 2004; Sperling, 2003; Leb, 1983). The following indicators allowed early metallurgists to identify bog iron ore deposits in the landscape: (i) withered grass, (ii) a wet environment, (iii) hygrophilous grass-dominated vegetation and (iv) reddish-brown solutions or depositions in nearby rivers and receiving waters (Koschke, 2002; Leb, 1983). The ore can be discovered through stoniness and compaction close to the surface, often at a depth of between 20 and 60 cm (Koschke, 2002; Evenstad, 1801; Sperling, 2003; Leb, 1983). In order to detect bog iron ore deposits under the subsurface wooden or metal sticks were stabbed into the ground (Evenstad, 1801; Leb, 1983; Oberrascher, 1939; Sperling, 2003).

Bog iron ores needed to have a minimum iron content of 55–60 mass% Fe (equivalent to 79–86 mass% Fe_2O_3) in order to be regarded as suitable by the iron smelters (Pleiner, 2000). Furthermore characteristic for bog iron ores is an often relatively high manganese content (Table 1; Graupner, 1982; Sperling, 2003). As Crew et al. (2011) states, the impact of manganese on the smelting process is subject of an ongoing debate and it has not finally been resolved yet whether manganese acts as a reduction catalyzer or is actually reduced to the bloom. Nevertheless considerable manganese contents in ores seem to be favorable for iron smelting: During the smelting process available manganese substitutes valuable iron as a fluxing agent for SiO_2 (Charlton et al., 2010; Iles, 2014), therefore ores containing considerable amounts of manganese with <70 mass% Fe_2O_3 could still be used for bloomery smelting (Heimann et al., 2001). Heimann et al. (2001) even states that manganese also lowers the critical CO_2 partial pressure, which enables iron smelting at lower process temperatures, also confirmed by Graupner (1982) and Iles (2014). As the MnO-FeO-SiO_2 ternary slag-diagram of Iles (2014) and Zhang et al. (2011) clearly shows, decreasing melting temperatures only correlate with increasing manganese contents for slags with >40 mass% fraction SiO_2. A ternary slag diagram for the slag samples of this case study, with liquidus temperatures after Iles (2014) is displayed in the appendix (Appendix, Fig. A.1). In case of iron slags below 40 mass% fraction SiO_2 in the MnO-FeO-SiO_2 ternary slag system increasing manganese contents would lead to an increase in the melting temperature (Iles, 2014; Zhang et al., 2011). In contrast the typically high porosity of bog iron ores clearly facilitates its reducibility during the smelting (Charlton et al., 2010). Again it is debatable whether a considerable phosphorous content – as it is often characteristic for bog iron ores (Table 1; Bauermeister and Kronz, 2006) – represents a disadvantage for prehistoric iron smelting attempts. While Graupner (1982), Bauermeister and Kronz (2006) and Sperling (2003) state that a considerable phosphorus content impairs the quality of the iron bloom as it favors the extraction of graphite in the bloom during the cooling-down process (Bauermeister and Kronz,

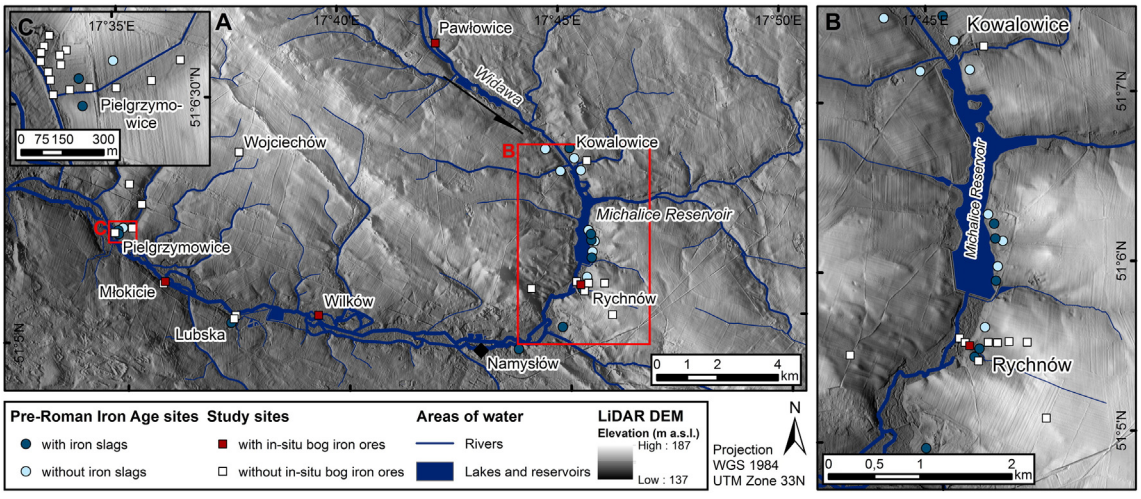

Fig. 2. A. Pre-Roman Iron Age sites and study sites investigated along the floodplain of the Widawa River; 2 B. Pre-Roman Iron Age and study sites in the vicinity of the Michalice Reservoir; 2 C. Pre-Roman Iron Age and study sites in the vicinity of Pielgrzymowice. Data sources: Fig. 2: A/B/C: Digital elevation model from LiDAR data 1 m horizontal resolution from CODGiK (2013); Rivers from TK25, 1: 25 000, map sheets 4871, 4872, 4971 and 4972 (TK25, 1886–1938); Lakes and reservoirs from CODGiK (2013); Archaeological sites from AZP (since 1978).

Please cite this article as: Thelemann, M., et al., Bog iron ore as a resource for prehistoric iron production in Central Europe — A case study of the Widawa catchment area in eastern ..., Catena (2016), http://dx.doi.org/10.1016/j.catena.2016.04.002

ARTICLE IN PRESS

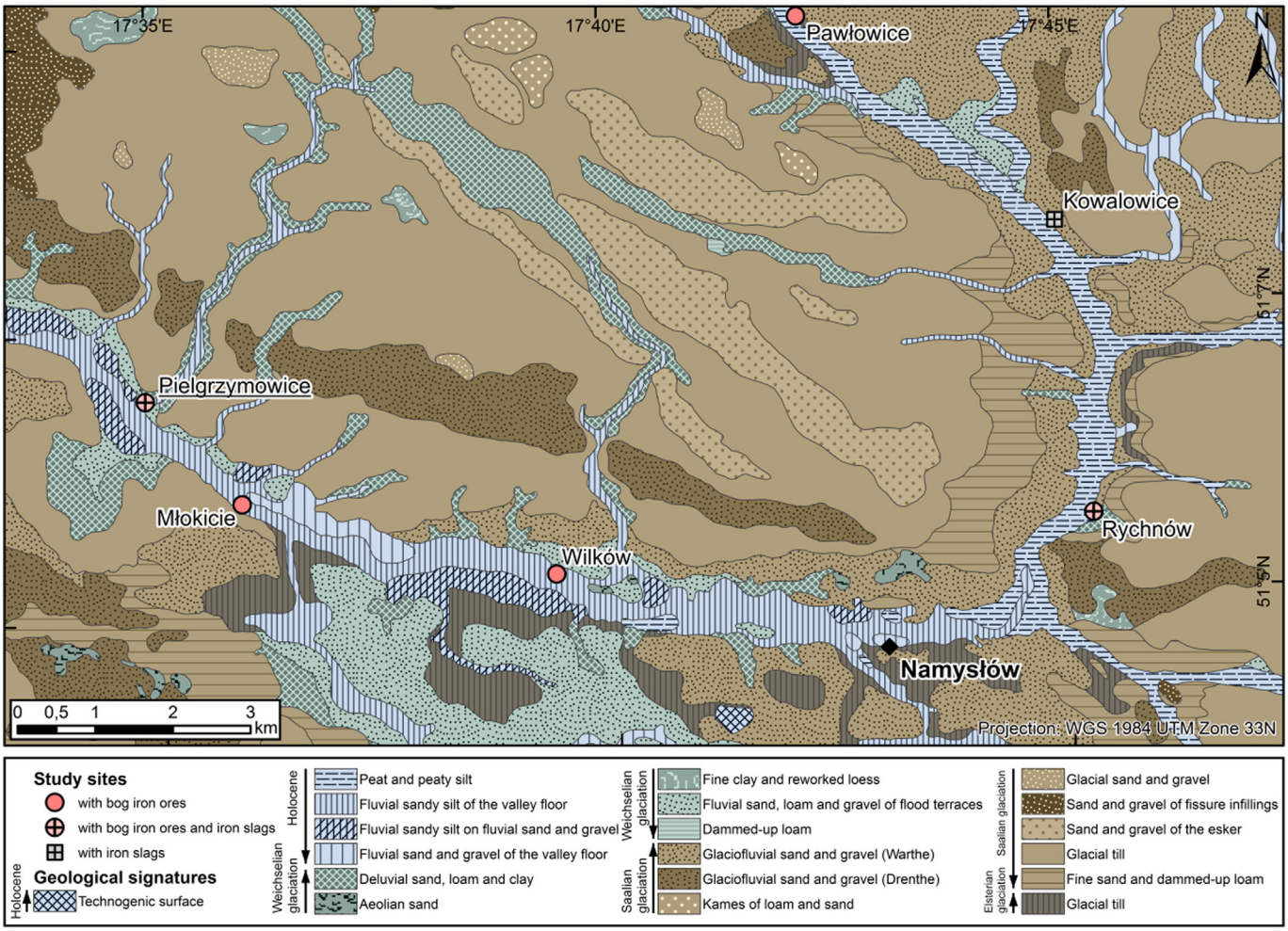

Fig. 3. Quaternary deposits. Data sources: Quaternary deposits from Geological detailed map 1 : 50 000 from Bartczak (1997), map sheet 0766; Cincio (1997), map sheet 0767.

2006), it is also seen as a hardening agent when alloyed (Buchwald, 2005). The behavior of phosphorus depends very much on the process temperatures during iron smelting (Buchwald, 2005). The higher the temperatures, the more phosphorus is transferred to the metal phase (Bauermeister and Kronz, 2006). Koschke (2002), Sperling (2003) and Heimann et al. (2001) state that calcium carbonate ($CaCO_3$) was therefore added to the smelting furnace in order to transfer higher phosphorus contents from bog iron ore to the slag. However, Bauermeister and Kronz (2006) state that the intentional adding of calcium carbonate in Lower Saxony, Germany, cannot be confirmed since it was not possible for the early blacksmiths to conduct these admixtures in exact measures during closed iron smelting processes. In principle the frequent occurrence of calcium-oxide in iron slags can also be explained by the presence of considerable carbonate or calcium-oxide contents in the exploited ores (Graupner, 1982; Krempler et al., 2004), furnace-lining material (Heimann et al., 2001) or charcoal ash (De Rijk, 2003).

1.2. Study area

The study area is located in the eastern part of Lower Silesia, Voivodeship Opole (Poland), in the catchment area of the Widawa River, a tributary of the Oder River (Fig. 1B). To the north the area is bound by the Silesian Ridge (Wał Trzebnicki), which represents the terminal moraine of the Warthe stadium of the Saalian glacial period (Rössner, 1998), while the Oder glacial valley forms the southern boundary (Fig. 1B). A cluster of prehistoric iron slag sites is located in this area, as revealed by a countrywide archaeological survey (Figs. 1B and 2; Archeologiczne Zdjęcie Polski, since 1978). The majority of these sites are situated in the vicinity of the Michalice reservoir, which was constructed in 2001 (Wiatkowski et al., 2010).

Geologically speaking, the study area belongs to the Pleistocene Old Drift landscape, which is – especially on the plateaus – dominated by Saalian glacial till deposits, but is also characterized by glacial deposits

Table 3
Setting, study sites and extraction methods.

Setting	Study site	Sample ID	Sample type	Extraction method
	Rychnów	bio01-1–bio04-1	Bog iron ore	Percussion drilling
In-situ	Pawłowice	bio12-1–bio13-1	Bog iron ore	Pürckhauer sondage
(sediment sequence)	Młokicie	bio14-1, bio17-1–bio21-2	Bog iron ore	Pürckhauer sondage/soil profile
	Wilków	bio22-1	Bog iron ore	Percussion drilling
	Pielgrzymowice	bio05-1–bio11-2, slag11-1–slag19-2	Bog iron ore/iron slag	Archaeological/geographical survey
Ex-situ	Młokicie	bio15-1–bio16-3	Bog iron ore	Geographical survey
(surface finds)	Rychnów	slag01–slag10-1	Iron slag	Archaeological survey
	Kowalowice	slag20-1–slag22-1	Iron slag	Archaeological survey

Please cite this article as: Thelemann, M., et al., Bog iron ore as a resource for prehistoric iron production in Central Europe — A case study of the Widawa catchment area in eastern ..., Catena (2016), http://dx.doi.org/10.1016/j.catena.2016.04.002

dating back to the Elsterian glacial period (Fig. 3; Bartczak, 1997; Cincio, 1997). The climate is a cold temperate, always humid continental Dfb climate with warm summers (Kuttler, 2009; Climate-Data.org, 1982–2012), average monthly temperatures of between −2 and 18 °C and annual precipitation of between 500 and 600 mm (Pelzer, 1991; Rössner, 1998; Climate-data.org, 1982–2012). Pedologically the study area is characterized by chernozems on the western plateaus and acidic cambisols on the eastern plateaus, podzoluvisols on the slopes and alluvial soils along the floodplain (Conrads, 1994; Pawlak, 1997, map sheet 28). The focus of this case study was set on six different sites in the Widawa catchment area (Fig. 1B).

2. Material and methods

In late summer 2013 and 2014 two field campaigns were conducted. The methodological approach included archaeological and geographical field methods, such as archaeological surveys, Pürckhauer sondages, percussion drillings using a Wacker drilling hammer (BHF 30 S) and the recording of soil profiles in order to characterize the archaeological sites and to extract bog iron ores and slags for geochemical and mineralogical analyses. Analyzed ores and slags originate from in-situ (sediment sequences from drillings and soil profiles) and ex-situ (surveys) contexts (Table 3). All slag samples originate from prehistoric slag sites dedicated to the pre-Roman Iron Age and the early Roman period by the AZP (since 1978). In the laboratory bog iron ore and slag pieces larger than 5 cm in diameter were divided into up to three subsamples. This procedure resulted in 35 bog iron ore and 28 iron slag subsamples. A detailed overview of sampling strategy and setting is given in the Appendix (Table A.1).

As a preprocessing step for elemental and mineralogical measurements all samples were homogenized, using a vibratory disc mill with an agate grinding set for 3 min, and dried for eight hours at 105 °C, and at below 60 °C prior to mineralogical analysis in order to avoid mineral alterations. The mineralogical composition was analyzed by X-ray powder diffractometry (XRD) using the Rigaku MiniFlex 600 X-Ray Diffractometer with a copper Kα-tube and a D/tex Ultra2 detector. The air-dried powdered samples (homogenized to ~1–10 μm particle diameter) were pressed without regulation into the sample holders and analyzed at 15 mA/40 kV (Cu kα) from 3° to 80° (2θ) with a goniometer step velocity of 0.02° steps and 0.5°/min^{-1}. The software X-Pert HighScore Version 1.0b by PHILIPS Analytical B.V. was used for a semi-quantitative identification and determination of the mineral composition. Five preprocessing steps were applied: (i) outliers were corrected; (ii) Kα_2-emissions were eliminated; (iii) the quartz $I = 100$ main peak ($d =$ 3.34 Å) was calibrated; (iv) reflex peaks were identified and (v) background noise was subtracted. For the assignment of the peaks to specific minerals standardized reference Powder Diffraction Files (PDF) of the ICDD (International Centre for Diffraction Data) were used. The mineralogical XRD measurements of bog iron ores and iron slags were interpreted very conservatively, with only clearly detectable peaks being taken into account. Because of the quantitative incomparability of peak intensities of different minerals the resulting evaluation of mineral contents was conducted semi-quantitatively according to Schütt (2004), using four classes.

For the elemental measurements of ores and slags, calibrated analyses, using a portable energy dispersive X-ray fluorescence spectrometer (*p*-ED-XRF), were applied. XRF provides a fast, non-consumptive, accurate and reproducible method to determine the elemental composition of rocks and sediments (Ramsey et al., 1995; De Vries and Vrebos, 2002; Jenkins, 1999) and is also a method applied for elemental analyses of bog iron ores and iron slags (Joosten et al., 1998; Kaczorek et al., 2004; Rzepa et al., 2009; Heimann et al., 2001; Blakelock et al., 2009). For calibration, selected sample material from Silesia was first analyzed at the Laboratory of Materials Science at the German Mining Museum Bochum (DBM) in order to obtain internal standard calibration material for the *p*-ED-XRF analyses. Eight selected bog iron ore samples and four selected iron slag samples from Silesia, as well as one bog iron ore sample from Heinersbrück, Germany and four iron slag samples from La Esterella, Majal del Toro and Mina de San Pedro, Spain, were analyzed with inductively coupled plasma mass spectrometry (ICP-MS) using the Thermo Scientific Element XR at the DBM. The results of the ICP-MS analysis are shown in Tables A.2 and A.3 in the Appendix. The samples from Spain with relatively high iron contents and the samples from Heinersbrück with relatively low iron contents were used as additional internal standard material (Appendix, Tables A.2 and A.3). Supplementary information on the measurement procedure at the DBM is provided in the Appendix (Section 1). With the internal laboratory standards obtained at the DBM, the *p*-ED-XRF analyses of the samples from Silesia were performed at the Freie Universität Berlin using a portable Thermo Fisher Scientific Analyticon NITON XL3t *p*-ED-XRF equipped with a CCD-camera, a semiconductor detector with an Ag-anode. The following filters were applied: a main filter with 50 kV, a low filter with 15/20 kV, a light filter with 8 kV and a high filter with 50 kV. The X-ray power is limited to 2 watts. For the measurement about 4 g of the powdered samples were placed in plastic cups and sealed with mylar foil (with a thickness of 0.4 μm). The prepared sample cups were placed on the *p*-ED-XRF and measured for 120 s with different filters for the detection of specific elements. In order to use the internal laboratory standards measured at the DBM by ICP-MS for calibration of the *p*-ED-XRF measurements, each of the internal laboratory standard samples was measured four times without calibration. The mean values were then plotted against the reference values in order to calculate a calibration function with a linear correlation coefficient as a quality measure. Outliers that distinctly impaired the coefficient were excluded from the calibration. Due to the differences in the chemical composition the standards from Spain were only used for the calibration of iron in the slags from Silesia. The high iron content of this internal standard material allows to measure reproducible results. All the calibration internal standard values used (Tables A.2 and A.3) and the correlation coefficients for the *p*-ED-XRF calibration (Table A.4) are presented in the Appendix. According to this procedure, only elements that were successfully calibrated with a correlation coefficient higher than $R = 0.80$ were considered for the measurements of ores and slags. A calibrated measurement was conducted for nine elements: iron (Fe), silicon (Si), manganese (Mn), calcium (Ca), phosphorus (P), potassium (K), barium (Ba) and titanium (Ti). During the evaluation of the results a review was conducted if the measured values exceeded four times the standard deviation of the measuring error and if the highest sample measurement was not exceeded by the internal standard material. Due to the clear linear correlation between the standard reference materials and the XRF-results all calibrated results were taken into account for the following statistical analyses and interpretation even if the values of the reference material were exceeded for single samples and single elements. The calibrated *p*-ED-XRF results of the bog iron ores and iron slags were initially displayed as element mass percentages. In accordance with comparative studies (Tables 1 and 2), the element contents were subsequently converted to oxides using standard conversion factors based on the molar mass, whereby the iron contents of oxidized bog iron ores were converted to Fe_2O_3 and the reduced iron slags were converted to FeO (Joosten et al., 1998; Puttkammer, 2012; Sperling, 2003).

The TIC and TOC contents were deduced from the loss on ignition (LOI) measured at 550 °C and 900 °C with the Thermo Scientific M110 Muffle Furnace according to Dean (1974), using a conversion factor of $1 * 1.72^{-1}$ from LOI550 to TOC and $1 * (44 * 100)^{-1} * 0.12$) from LOI900 to TIC (Dean, 1974). Every result for each sample was summed in order to calculate the total of the elemental composition as a quality measure.

Using the results of the elemental analyses of iron slags from the study area the reducible iron index ($RII = 2.39 * SiO_2/(FeO + MnO)$) was calculated according to Charlton et al. (2010) in order to draw conclusions on the reduction efficiency of the smelting process (Table 5). Furthermore the iron and silicon contents, which typically represent the main elements, were plotted against each other in a total least

Please cite this article as: Thelemann, M., et al., Bog iron ore as a resource for prehistoric iron production in Central Europe — A case study of the Widawa catchment area in eastern ..., Catena (2016), http://dx.doi.org/10.1016/j.catena.2016.04.002

Table 4
Results of the mineralogical XRD and elemental *p*-ED-XRF analyses of bog iron ore samples for the study sites along the floodplain of the Widawa River.

Sample Name	**Location** Study site Setting	**Quartz**	**Goethite**	**Hematite**	**Magne–tite**	**Mag–hemite**	**Siderite**	**Pyrite**	**Ortho–clase**	**Calcite**	Fe_2O_3	SiO_2	MnO	CaO	P_2O_5	Al_2O_3	K_2O	BaO	TiO_2	**Remain. Oxides**	**TIC LOI (900 °C)**	**TOC LOI (550 °C)**	**Tot. LOI (900 °C)**	**SUM**
		Results from calibrated energy dispersive portable XRF measurements																						
		[mass%]	[mass%]	[mass%]	[mass%]	[mass%]	[mass%]	[mass%]	[mass%]	[mass%]	[mass%]	[mass%]	[mass%]	[mass%]	[mass%]	[mass%]	[mass%]	[mass%]	[mass%]	[mass%]	[mass%]	[mass%]	[mass%]	[mass%]
bio01–1	Rychnów Alluvial fan (drilling)	++++	+++	+		+			++		55.9	19.4	1.5	1.7	4.7**	1.7	0.2	0.3	0.2	0.3	1.2	6.0	14.7	100.6
bio02–1		++++	+++	++	++	++				++	64.9**	13.7	0.4	2.2	4.7**	1.7	0.1	0.3	0.1	0.3	0.7	6.7	14.0	102.3
bio03–1		+++	+++	++	+	+				++++	59.2**	10.6	0.5	7.4**	6.9**	2.0	0.0*	0.3	0.2	0.3	1.2	6.1	15.0	102.4
bio04–1		+	++	+	+	+	+	+		++++	45.5	10.4	0.6	18.7**	3.6	3.4**	0.0*	0.1	0.1	0.5	3.8	7.0	26.2	109.0
bio05–1	Pielgrzymowice Slope (survey)	++++	++			+	+	+	+		51.4	20.1	1.0	2.7	3.8	2.6	0.5	0.1	0.1	0.2	0.6	7.1	14.3	96.8
bio05–2		++++	++	+	++		+	+	+		53.9	18.4	1.0	2.8	4.2**	2.7	0.5	0.1	0.2	0.2	0.6	7.8	15.8	99.7
bio06–1		++++	+++		+	+	++	++			53.6	18.9	1.0	2.5	3.7	2.7	0.5	0.1	0.2	0.2	1.0	6.2	14.5	98.0
bio07–1		++++	++	+	+	+	++		+		52.4	17.7	1.9	3.4	3.8	2.4	0.4	0.2	0.1	0.2	1.1	7.6	17.0	99.5
bio07–2		++++	++	+	+	+	+	+	+		46.5	17.4	4.4	6.4**	2.8	2.6	0.4	0.2	0.2	0.1	2.0	7.0	19.4	100.3
bio08–1		++++	+++	++						++	52.2	16.7	2.8	4.8	3.2	2.1	0.3	0.2	0.1	0.2	1.6	6.6	17.3	99.8
bio09–1	Vicinity of Pielgrzymowice (clearance cairn)	++++	+	+	+	+		+			32.0	36.2	2.4	1.1	2.4	2.0	0.5	0.4**	0.2	0.2	0.6	3.0	7.6	85.1
bio09–2		++++	++		+	+		+			23.6	43.6	2.5	1.0	1.8	2.3	0.7	0.4**	0.3**	0.2	0.6	2.6	6.5	82.7
bio10–1		++++	++		+	+					38.4	27.0	2.9	0.9	2.0	3.3**	0.7	0.4**	0.3**	0.2	0.8	3.7	9.2	85.3
bio10–2		++++	++	+	+	+					42.9	25.5	2.6	1.0	2.1	2.8	0.6	0.4**	0.3**	0.2	0.8	3.5	9.0	87.2
bio11–1		++++	++	+	+	+					33.0	35.3	1.4	1.0	2.0	2.1	0.4	0.2	0.2	0.1	0.6	3.3	8.0	83.6
bio11–2		++++	+								33.5	36.3	1.6	0.8	1.9	1.9	0.5	0.2	0.2	0.1	0.7	3.3	8.1	85.0
bio12–1	Pawłowice Slope (drilling)	++++	+	+	+				+		21.6	52.7	0.5	0.8	1.5	1.7	0.6	0.1	0.1	0.1	0.6	4.4	6.9	86.5
bio13–1		++++	+	+				+	+		25.8	44.1	1.9	1.3	2.6	3.5**	0.9	0.1	0.2	0.1	0.4	3.1	9.6	90.1
bio14–1	Młokicie Slope (drilling)	++++	+								23.8	52.1	2.5	1.9	3.2	1.8	0.6	0.03	0.1	0.1	0.8	4.5	10.6	96.6
bio15–1	Młokicie Riverbed (survey)	++++	+	+					+		33.3	41.1	3.3	1.5	2.3	1.9	0.5	0.1	0.1	0.1	0.6	4.7	10.3	94.5
bio15–2		++++	+	+				+	+		33.8	30.3	4.1	1.6	2.5	1.7	0.5	0.2	0.1	0.1	0.7	5.0	10.9	85.9
bio15–3		++++	+	+	+	+		+	++		32.7	29.6	5.7	1.9	2.2	2.1	0.4	0.2	0.2	0.1	0.7	5.3	11.7	86.9
bio16–1		++++	+	+	+	+		+	+		27.6	39.1	2.9	1.6	2.4	2.9	0.8	0.2	0.2	0.1	0.5	3.9	8.6	86.3
bio16–2		++++	+	+	+	+		+	+		34.6	29.5	2.6	1.6	2.7	2.8	0.6	0.2	0.2	0.1	0.6	4.7	10.1	85.1
bio16–3		++++	+	+	+	+	+	+	+		34.3	30.8	3.0	1.9	2.2	3.1	0.7	0.2	0.2	0.1	0.6	6.8	13.9	90.4
bio17–1	Młokicie Riverbank (soil profile)	++++	+	+	+			+	+		13.6	47.3	0.7	1.4	1.8	3.2	1.0**	0.1	0.2	0.1	0.4	4.6	9.3	78.5
bio18–1		++++	+	+	+				+		6.2	57.4**	1.4	1.1	1.6	2.5	0.9	0.1	0.2	0.1	0.3	1.9	4.4	75.7
bio18–2		++++	+	+	+			+	+		12.4	47.4	1.6	1.2	2.3	4.0**	1.0**	0.1	0.3**	0.1	0.4	3.3	7.1	77.6
bio19–1		++++	+	+	+			+	+		11.7	51.8	1.0	1.0	2.1	4.0**	1.2**	0.1	0.3**	0.1	0.5	4.3	9.2	82.4
bio19–2		++++	+	+	+			+	+		7.9	60.2	0.7	1.0	1.8	4.5**	1.3**	0.1	0.3**	0.2	0.4	3.4	7.2	85.10
bio20–1		++++	+	+	+			+	+		1.6	80.3**	0.1	0.7	1.8	3.9**	1.4**	0.1	0.2	0.1	0.3	1.5	3.5	93.7
bio20–2		++++	+	+	+			+	+		2.6	75.6**	0.2	0.7	2.4	4.1**	1.4**	0.1	0.2	0.1	0.3	1.9	4.4	91.8
bio21–1		++++	+	+	+			+	+		18.1	45.0	2.8	1.3	1.8	3.4**	1.0**	0.1	0.2	0.1	0.5	4.0	8.8	82.5
bio21–2		++++	+	+	+			+	+		15.8	45.6	2.9	1.3	1.7	3.6**	1.0**	0.1	0.3**	0.1	0.6	3.8	8.5	80.8
bio22–1	Wilków Floodplain (drilling)	++++	+								6.7	82.3	0.2	0.2	0.5	2.6	0.9	0.0	0.1	0.1	0.4	2.3	5.2	98.7
bio23–1	Heinersbrück, Germany	++++	+	+	+			+	+		22.4	53.4	0.8	1.8	4.7	3.0	0.7	0.1	0.2	0.1	0.4	4.8	9.7	96.9

++++ maximum counts per second +++ major components ++ minor components + traces *smaller than four times the standard deviation of the measuring error **higher than the highest standard measurement

Under Remain. oxides the uncalibrated XRF measurements of CeO_2, Sb_2O_3, SnO, CdO, Ag_2O, UO_2, Nb_2O_5, ZrO_2, Y_2O_3, SrO, Rb_2O, Bi_2O_3, PbO, Au_2O, SeO_3, As_2O_3, HgO, ZnO, CuO, NiO, CoO, Cr_2O, V_2O, Cl, SO_3 and MgO are summed.

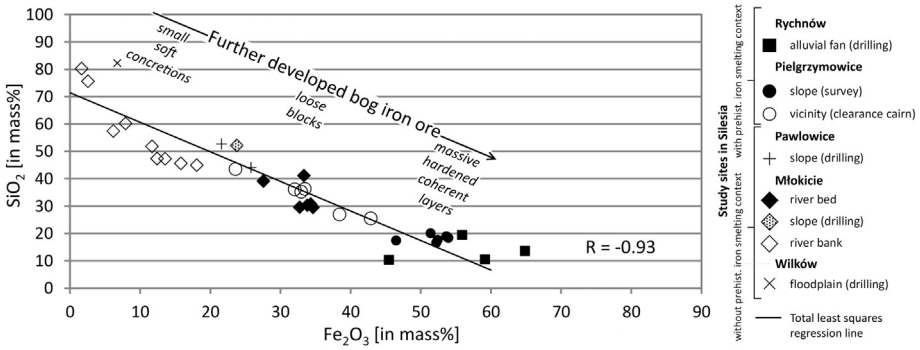

Fig. 4. Total least squares regression model of iron-hydroxide and silicon-dioxide in bog iron ores. [Further developed bog iron ores in regard to their iron and silicon contents (Table 4)].

squares regression model and correlation coefficients were calculated. In order to statistically compare the not-normally distributed results from the literature review (Tables 1 and 2) and the study area, nonparametric 1- and 2-tailed *U* tests of iron contents in ores and slags from both datasets were conducted after Wilcoxon, Mann and Whitney in order to compare their magnitude (Wilcoxon, Mann and Whitney cited after Rinne, 2008). Furthermore a multivariate principal component analysis (PCA) was conducted from each correlation matrix of the calibrated oxide measurements with an eigenvalue >1 in order to investigate coherences in the elemental composition and to analyze, structure, summarize and simplify the datasets (Fahrmeir et al., 1996; Hartmann and Wünnemann, 2007; Charlton et al., 2012).

3. Results

3.1. Mineralogical and elemental composition of the bog iron ores

Mineralogically, the analyzed bog iron ore samples mainly consist of quartz (SiO_2), while two samples (bio03-1 and bio04-1) are dominated by calcite (Table 4). Among the iron minerals goethite (α-FeO(OH) prevails, while magnetite (Fe_3O_4), hematite (Fe_2O_3), maghemite (γ-Fe_2O_3), orthoclase ($K[AlSi_3O_8]$) and pyrite (FeS_2) occur frequently in traces. Additionally, in some samples traces of siderite ($FeCO_3$) were detected (Table 4). The diffractograms of representative bog iron ore samples are shown in the Appendix (Fig. A.4 to A.8).

The oxide composition of sampled initial and developed bog iron ores is mainly comprised of iron (III) oxide (Fe_2O_3) and silicon-dioxide (SiO_2) with contents between 1.6 and 64.9 mass% Fe_2O_3 (sample bio20-1 and bio02-1; $\bar{x} = 31.5$ mass% Fe_2O_3; $n = 35$), and between 10.4 and 82.3 mass% SiO_2 (bio04-1 and bio22-1; $\bar{x} = 37.4$ mass% SiO_2; $n = 35$) (Table 4). Apart from Fe_2O_3 and SiO_2, the oxides CaO (max. 18.7 mass%), P_2O_5 (max. 6.9 mass%), MnO (max. 5.7 mass%) and Al_2O_3 (max. 3.4 mass%) are also present in considerable amounts in the elemental composition of the ores, while K_2O (max. 1.4 mass%), TiO_2 (max. 0.4 mass%) and BaO (max. 0.4 mass%) represent minor contents (Table 4). The TIC contents in the sampled ores vary between 0.3 and 3.8 mass% ($\bar{x} = 0.8$ mass%; $n = 35$), while TOC contents vary between 1.5 and 7.8 mass% ($\bar{x} = 4.6$ mass%; $n = 35$) (Table 4).

For all samples a linear correlation with a correlation coefficient of $R = -0.93$ was detected between iron and silicon (Fig. 4). With values between 45.5 and 64.9 mass% Fe_2O_3 ($\bar{x} = 56.4$ mass% Fe_2O_3; $n = 4$), the samples from Rychnów show the highest Fe_2O_3 contents, followed by samples from Pielgrzymowice with between 46.5 and 53.9 mass% Fe_2O_3 ($\bar{x} = 51.7$ mass% Fe_2O_3; $n = 6$) originating from the archaeological survey, and with between 23.6 and 42.9 mass% Fe_2O_3 ($\bar{x} = 33.9$ mass% Fe_2O_3; $n = 6$) originating from a nearby clearance cairn (Fig. 1B; Table 4). The other bog iron ore sites of the riverbed and drilling at Młokicie and the drilling at Pawłowice reach mean Fe_2O_3 contents of 32.7 ($n = 6$), 23.8 ($n = 1$), and 23.7 ($n = 2$) mass% Fe_2O_3. At the remaining sites of Młokicie (riverbank) and Wilków (floodplain) the samples show mean iron contents of 10.0 ($n = 9$) and 6.7 ($n = 1$) mass% Fe_2O_3 (Fig. 1B; Table 4).

The PCA of the elemental composition of bog iron ores resulted in nine principal components (PCs). The first two PCs account for 52.1

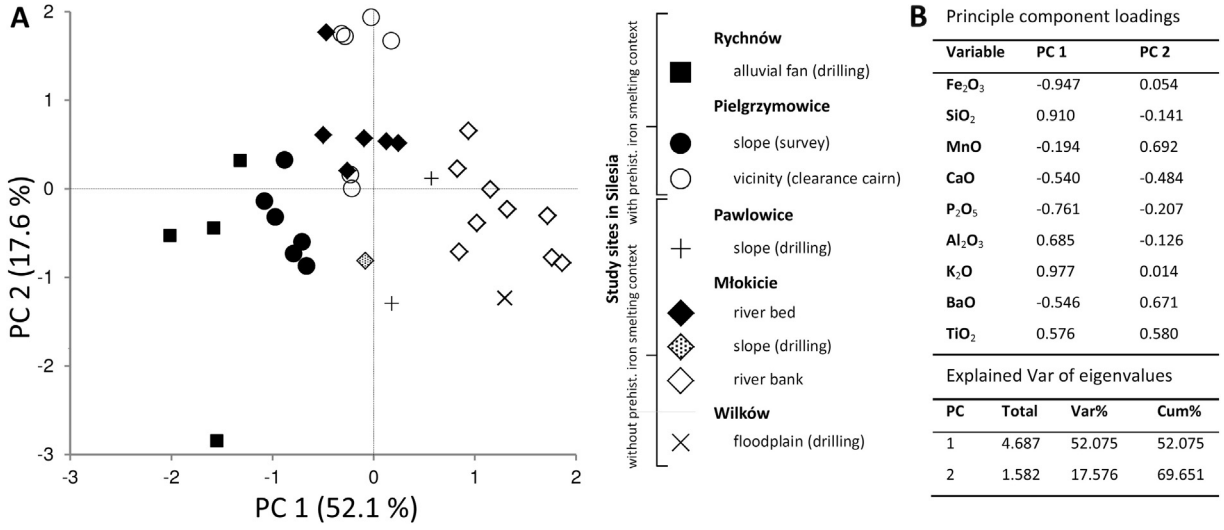

B Principle component loadings

Variable	PC 1	PC 2
Fe_2O_3	-0.947	0.054
SiO_2	0.910	-0.141
MnO	-0.194	0.692
CaO	-0.540	-0.484
P_2O_5	-0.761	-0.207
Al_2O_3	0.685	-0.126
K_2O	0.977	0.014
BaO	-0.546	0.671
TiO_2	0.576	0.580

Explained Var of eigenvalues

PC	Total	Var%	Cum%
1	4.687	52.075	52.075
2	1.582	17.576	69.651

Fig. 5. A. PC-plot of PC 1 and 2 of the major oxide concentrations in bog iron ores; 5 B. Principal component loadings of the PCA on bog iron ores. [Reduction efficiency of the smelting process calculated according to Charlton et al., 2010 (Table 5).]

Table 5
Results of the mineralogical XRD and elemental *p*-ED-XRF analyses of slag samples for the study sites along the floodplain of the Widawa River.

Sample Name	Location Study site Setting	Faya-lite	Quartz	Wüs-tite	Goethite	Hema-tite	Magne-tite	Maghe-mite	Side-rite	Pyrite	Ortho-clase	Augite	FeO	SiO_2	MnO	CaO	P_2O_5	Al_2O_3	K_2O	BaO	TiO_2	Remain. oxides (900 °C)	TIC LOI (550 °C)	TOC LOI (900 °C)	Tot. LOI	SUM	*RII* ***
													Results from calibrated energy dispersive portable XRF measurements														
													[mass%]	[mass%]	[mass%]	[mass%]	[mass%]	[mass%]	[mass%]	[mass%]	[mass%]	[mass%]	[mass%]	[mass%]	[mass%]		
slag01–1	Rychnów Slope (survey)	++++	+	++	+	+	++	++	+	+	+		69.1	22.3	5.8	1.7	0.6	3.7**	0.5	0.1*	0.1	0.3	0.0	0.0	0.0	104.2	0.71
slag02–1		++++	+	+	+	+	+++	++	+	+			56.1	26.5	8.4**	3.8	0.6	4.0**	1.0	0.1	0.1	0.3	0.0	0.0	0.0	101.0	0.98
slag03–1		++++		++	+	+	++	+	+	++			54.3	26.7	8.2**	3.3	0.8	4.6**	1.2**	0.1	0.2	0.4	0.0	0.0	0.0	99.7	1.02
slag03–2		++++	+	+	+	+	+		+	+	++		58.1	27.7	5.7	2.1	0.6	5.3**	1.0	0.1*	0.2	0.3	0.0	0.0	0.0	101.1	1.04
slag04–1		++++	+	++			++						54.8	26.6	7.5	2.9	0.7	4.6	1.1	0.1	0.3	0.4	0.0	0.0	0.0	98.9	1.02
slag05–1		++++		++	+	+	++	+	+	+	+		62.1	24.7	7.0	1.3	0.5	3.9**	0.8	0.1	0.2	0.3	0.0	0.0	0.0	100.9	0.85
slag06–1		++++		+++			+		+				61.7	24.6	6.9	1.3	0.6	4.1	0.8	0.1	0.2	0.3	0.0	0.0	0.0	100.6	0.86
slag07–1		++++	+	++	+	+	+	+	+	++			62.8	26.2	5.8	1.4	0.6	3.6	0.9	0.1*	0.1	0.3	0.0	0.0	0.0	101.8	0.91
slag08–1		++++	+	+++		+	+	++	++	+	+		71.2	23.0	5.2	1.2	0.6	3.7**	0.5	0.1	0.1	0.4	0.0	0.0	0.0	105.8	0.72
slag09–1		++	++++	++	+	+	++	++	+	+	+		67.0	20.3	4.7	1.7	1.1	3.4	0.4	0.0*	0.1	0.3	0.0	0.0	0.0	99.1	0.68
slag10–1		++++		++		+	++	+	+	+			59.5	25.8	7.0	2.6	0.9	4.4	1.1**	0.1	0.2	0.3	0.0	0.0	0.0	101.8	0.93
slag11–1	Pielgrzymowice Slope (survey)	++	++		+	++	++	++	++	+	++	++++	11.7	45.6	0.1	11.0**	0.9	9.3**	1.5**	0.2	0.9**	5.8	0.0	0.0	0.0	87.1	9.24
slag12–1		++++	+	+++			++						57.2	26.2	3.2	4.4	0.6	5.7**	0.8	0.1	0.3	0.3	0.0	0.0	0.0	98.8	1.04
slag13–1		+++	++++	++	+	+	++	+	+	+	+		71.6	28.9	0.8	1.3	2.9	2.1	0.4	0.1	0.1	0.3	0.0	0.0	0.0	108.4	0.95
slag14–1		++++	+	+	+	+	+	+			+		60.7	27.0	4.9	1.5	5.1**	2.6	0.6	0.4**	0.3	0.4	0.0	0.0	0.0	103.4	0.98
slag15–1		++++	+	+	+	+	++	+	+	+	+		48.7	40.7	3.3	1.9	2.4	2.4	0.8	0.3	0.2	0.2	0.0	0.0	0.0	100.9	1.87
slag16–1		++++		++	+	+	++	++	+	+			56.8	25.7	3.2	4.5	0.7	5.9**	0.8	0.1	0.3	0.4	0.0	0.0	0.0	98.2	1.02
slag16–2		++++		++	+	+	++	++	+	+			56.9	26.5	3.2	4.5	0.7	6.1**	0.9	0.1*	0.2	0.4	0.0	0.0	0.0	99.3	1.05
slag17–1		++++	+++	+++			++			++			51.0	30.6	3.6	5.0	0.5	5.9**	0.9	0.1	0.4**	0.3	0.0	0.0	0.0	98.2	1.34
slag18–1		+++	++++	++	+	+	+	+			+		68.1	30.3	0.4	2.0	4.8**	2.2	0.4	0.1	0.1	0.3	0.0	0.0	0.0	108.7	1.06
slag18–2		+++	+++	++	+	+	+	+	+	+	+		72.0	22.1	0.5	2.3	6.4**	2.1*	0.3	0.1	0.1	0.3	0.0	0.0	0.0	106.2	0.73
slag19–1		++++	+	++		+	++	++	+	+	+		51.5	29.1	3.8	5.2**	0.6	6.9**	1.0	0.1*	0.3	0.3	0.0	0.0	0.0	98.6	1.26
slag19–2		++++		++	+	+	+	++	+	+	++		51.6	27.4	3.8	5.2	0.5	6.2**	1.0	0.1	0.3	0.4	0.0	0.0	0.0	96.5	1.18
slag20–1	Kowalowice Slope (survey)	++++	++	+	+	+	++	+		++	+		57.2	23.1	8.6**	2.6	7.3**	1.9	0.7	0.8**	0.5**	0.4	0.0	0.0	0.0	102.9	0.84
slag20–2		++++	++	++	+	+	+	+	+	+	+		61.8	22.0	8.3**	2.5	7.0**	2.1	0.6	0.8**	0.5**	0.3	0.0	0.0	0.0	105.9	0.75
slag21–1		++++	+	++	+	+	++	+	+	+	+		59.4	27.2	7.3	2.0	0.6	4.6	1.0	0.1	0.2	0.4	0.0	0.0	0.0	102.8	0.97
slag21–2		++++	+	++	+	+	++	+	+	++	+		60.1	26.4	7.2	2.1	0.5	4.5	1.0	0.1	0.2	0.3	0.0	0.0	0.0	102.4	0.94
slag22–1		++++	++		++	++	+	++	+	++	++	++	16.2	44.9	0.0*	6.8**	0.5	12.4**	2.3**	0.1	1.1**	0.6	0.0	0.0	0.0	84.9	6.62
slagMR1	La Esterella 1, Spain	–	–	–	–	–	–	–	–	–	–	–	73.3	15.4	0.0*	0.7	0.0*	0.8*	0.0*	0.0*	0.0*	0.7	0.0	0.0	0.0	91.1	0.50
slagMR2	La Esterella 2, Spain	–	–	–	–	–	–	–	–	–	–	–	79.6	6.4	0.0*	0.6	0.0*	0.9*	0.0*	0.0*	0.0*	0.2	0.0	0.0	0.0	87.6	0.19
slagMR3	Majal del Toro 2, Spain	–	–	–	–	–	–	–	–	–	–	–	5.2	47.8	0.0*	0.3	0.0*	1.7	0.0*	0.0*	0.0*	20.4	0.0	0.0	0.0	75.4	21.97
slagMR4	Mina de San Pedro 1, Spain	–	–	–	–	–	–	–	–	–	–	–	23.9	37.0	0.0*	0.3	0.0*	0.9*	0.0*	0.0*	0.0*	20.4	0.0	0.0	0.0	82.5	3.70

++++ maximum counts per second +++ major components ++ minor components + traces *smaller than four times the standard deviation of the measuring error **higher than the highest standard measurement
***Reducible Iron Index (according toCharlton et al., 2010)
Under Remain. oxides the uncalibrated XRF measurements of CeO_2, Sb_2O_3, SnO, CdO, Ag_2O, UO_2, Nb_2O_5, ZrO_2, Y_2O_3, SrO, Rb_2O, Bi_2O_3, PbO, Au_2O, SeO_3, As_2O_3, HgO, ZnO, CuO, NiO, CoO, Cr_2O, V2O, Cl, SO_3 and MgO are summed.

Please cite this article as: Thelemann, M., et al., Bog iron ore as a resource for prehistoric iron production in Central Europe — A case study of the Widawa catchment area in eastern ..., Catena (2016), http://dx.doi.org/10.1016/j.catena.2016.04.002

and 17.6% of the total variance (Fig. 5A). According to the values of the PC loadings, PC 1 particularly represents the oxides K_2O, Fe_2O_3, SiO_2, P_2O_5 and Al_2O_3, whereas PC 2 mainly represents the oxides MnO and BaO (Fig. 5B). The resulting plot of PC 1 against PC 2 (Fig. 5A) is evenly scattered, while the point clouds of the samples from different study sites hardly overlap, apart from the clearance cairn at Pielgrzymowice and the riverbed at Młokicie (Fig. 5A).

The statistical comparison between the iron contents in bog iron ores from the literature review and the study area, applying the 2-tailed *U* test after Wilcoxon, Mann and Whitney with the null hypothesis that the distributions of both datasets come from the same population, resulted in a *p*-value of $P = 0.001$, which rejects the null hypothesis of $P > 0.05$ with a significance level of $\alpha = 0.05$. A subsequent 1-tailed *U* test with the null hypothesis that the comparative studies tend to have larger values, resulted in a *p*-value of $P = 0.001$, which accepts the null hypothesis of $P < 0.05$ with a significance level of $\alpha = 0.05$.

3.2. Mineralogical and elemental composition of the iron slags

All collected slags are greyish in color, show magnetic properties and do not contain TIC and TOC contents in terms of inorganic carbon (e.g. $CaCO_3$), humus or plant material (Table 5). Mineralogically, most of these samples mainly consist of fayalite (Fe_2SiO_4), only four slag subsamples (slag09-1, slag13-1, slag18-1 and slag18-2) consist mainly of quartz (SiO_2) and one of augite ($(Ca,Mg,Fe)_2Si_2O_6$; slag11-1). A major to minor component in the iron slags is wüstite (FeO). Magnetite (Fe_3O_4) and maghemite (γ-Fe_2O_3) mostly occur as minor components, whereas pyrite (FeS_2), orthoclase ($K[AlSi_3O_8]$), siderite ($FeCO_3$), hematite (Fe_2O_3) and goethite (α-FeO(OH)) often occur in traces (Table 5). Diffractograms of representative iron slag samples are shown in the Appendix (Fig. A.9 to A.13).

The elemental composition of the sampled slags mostly consists of FeO (11.7 to 72.0 mass% FeO; $\bar{x} = 56.8$ mass% FeO; $n = 28$) and SiO_2 (20.3 to 45.6 mass% SiO_2; $\bar{x} = 45.6$ mass% SiO_2; $n = 28$) (Table 5). Similar to the bog iron ores, the FeO and SiO_2 contents in the iron slags also show a linear correlation with a correlation coefficient of $R = -0.86$: the higher the FeO content, the lower the SiO_2 content (Fig. 6). The iron slags from Rychnów with values between 54.3 and 71.2 mass% FeO ($\bar{x} = 61.5$ mass% FeO; $n = 11$) show the highest iron contents, followed by the samples from Pielgrzymowice with between 11.7 and 72.0 mass% FeO ($\bar{x} = 54.8$ mass% FeO; $n = 12$), and Kowalowice with between 16.2 and 61.8 mass% FeO ($\bar{x} = 50.9$ mass% FeO; $n = 5$) (Table 5). Furthermore Al_2O_3 (max. 12.4 mass%), CaO (max. 11.0 mass%), MnO (max. 8.6 mass%) and P_2O_5 (max. 7.3 mass%) are significant elements in the composition of the sampled iron slags, while K_2O (max. 2.3 mass%), TiO_2 (max. 0.9 mass%) and BaO (max. 0.8 mass%) only contribute minor contents (Table 5). The *RII* (Table 5), lies between 0.7 and 1.9 with two outliers reaching 6.6 and 9.2. Most samples show an *RII* smaller than 1 and depending on the iron, silicon and manganese contents the *RII* (Table 5) shows a high negative correlation of $R = -0.91$ with the iron contents in the slags (Table 5; Fig. 6).

Throughout the PCA of the elemental slag composition nine PCs with loadings for each element were calculated. PC 1 accounts for 57.9% and PC 2 covers 21.7% of the total variance. While PC 1 with FeO, Al_2O_3, K_2O, CaO, TiO_2 and SiO_2 represents most of the selected oxides, PC 2 particularly represents the oxides BaO and P_2O_5 (Fig. 7B). The resulting scatterplot (Fig. 7A) shows relatively wide overlapping point clouds for the study sites of Pielgrzymowice and Kowalowice, while the point cloud of Rychnów is relatively concentrated.

The statistical comparison between the iron contents in iron slags from the literature review and the study area, applying the 2-tailed *U* test with the null hypothesis that the distributions of both datasets come from the same population, resulted in a *p*-value of $P = 0.019$, which rejects the null hypothesis of $P > 0.05$ with a significance level of $\alpha = 0.05$. The 1-tailed *U* test with the null hypothesis that the comparative studies tend to have larger values, resulted in a *p*-value of $P = 0.009$, which accepted the null hypothesis of $P < 0.05$ with a significance level of $\alpha = 0.05$.

4. Discussion

4.1. Bog iron ores

The sampled bog iron ores in the study area – with varying iron and silicon contents – come from in-situ samples (Rychnów, Pawlowice, Młokicie and Wilków) as well as from surface finds (Pielgrzymowice and Młokicie) (Tables 3 and 4). At the prehistoric smelting site of Pielgrzymowice and the study sites of Lubska, Kowalowice and Wojciechów, in-situ ore deposits were not detected (Fig. 2). Bog iron ore finds from the study area originate from the wetter margins of the Widawa floodplain, as is also described in general by Wünsche (2007) and for Lusatia (Germany) by Koschke (2002). Outside the lowlands no bog iron ores or iron concretions were detected in any of the conducted drillings (Fig. 2). The Saalian glacial till plateaus (Fig. 3) probably function as the main source of iron and manganese, which were relocated with the groundwater flux (Graupner, 1982; Oberrascher, 1939), whereas the Pleistocene glaciofluvial sands of the valley margins of the study area (Fig. 3) provide typical favorable conditions for bog iron ore formation (Oberrascher, 1939).

The rare occurrence and fragmented distribution of present day bog iron ore deposits reflect former mining activities as well as agriculture and melioration measures. These activities not only inhibit neoformations but also degrade former deposits (Graupner, 1982; Leb, 1983; Puttkammer, 2012), which impedes a complete reconstruction of the prehistoric situation. Additionally, the dryer climate compared to that of the main bog iron ore formation period in the Atlantic (Graupner, 1982) negatively affected recent bog iron ore neoformations (Wünsche, 2007). Therefore, today's deposits often represent only relicts of the former distribution (Graupner, 1982).

Mineralogically – besides quartz (SiO_2), orthoclase ($K[AlSi_3O_8]$) and calcite ($CaCO_3$) – the collected bog iron ores from the study area consist of a number of iron minerals that are typical for (bog) iron ores, such as

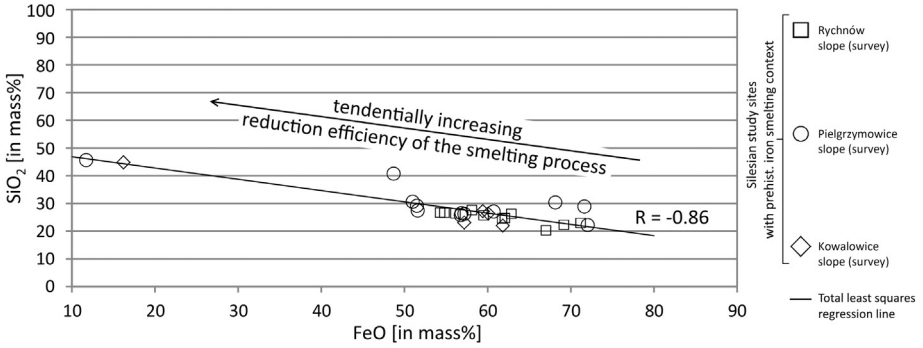

Fig. 6. Total least squares regression model of iron-oxide and silicon-dioxide in iron slags.

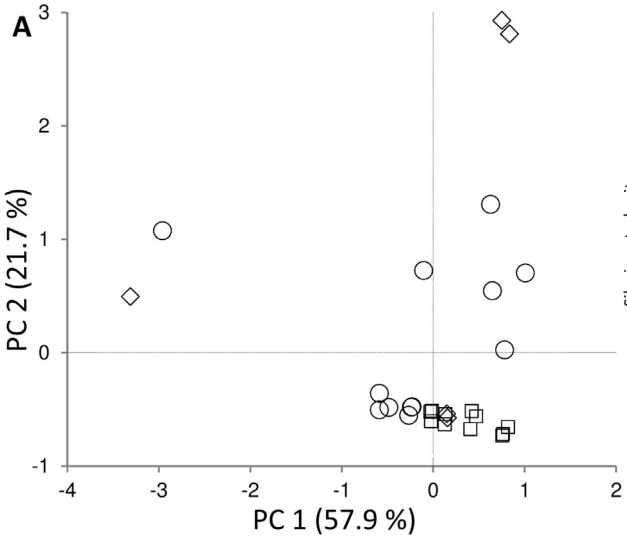

B Principle component loadings

Variable	PC 1	PC 2
FeO	0.964	-0.185
SiO_2	-0.850	0.152
MnO	0.449	-0.042
CaO	-0.880	0.107
P_2O_5	0.394	0.867
Al_2O_3	-0.933	-0.228
K_2O	-0.885	-0.073
BaO	0.185	0.940
TiO_2	-0.860	0.434

Explained Var of eigenvalues

PC	Total	Var%	Cum%
1	5.210	57.889	57.889
2	1.953	21.697	79.586

Fig. 7. A. PC-plot of PC 1 and 2 of the major oxide concentrations in iron slags; 7 B. Principal component loadings of the PCA on iron slags.

goethite (α-FeO(OH)), magnetite (Fe_3O_4), hematite (Fe_2O_3), maghemite (γ-Fe_2O_3), siderite ($FeCO_3$) and pyrite (FeS_2) (Banning, 2008; Graupner, 1982). Other iron minerals typical for bog iron ores, such as lepidocrocite ($Fe^{3+}O(OH)$) and vivianites ($Fe_3^{2+}(PO_4)_2 \times 8H_2O$) (Krempler et al., 2004; Banning, 2008; Sitschick et al., 2005), were not detected in the XRD analyses (Table 4). Especially considerable hematite and maghemite contents (bio02-1, bio03-1; Table 4), but also notable goethite and magnetite contents (bio01-1, bio05-2; Table 4), indicate a further developed iron mineral formation (Zwahr et al., 2000). Characteristic for the samples from the in-situ bog iron ore site of Rychnów (bio02-1, bio03-1, bio04-1; Table 4) is the occurrence of calcite ($CaCO_3$) minerals, which is interpreted as resulting from increasing temperature or decreasing hydrostatic pressure that led to the (near-surface) precipitation of carbonates from the groundwater flux (Correns, 1969). Since the applied XRD analysis measures the diffraction reflexes of crystal structures, this method provides hardly any information on non-crystalline, amorphous substances (Last, 2001), such as amorphous iron-hydroxides (e.g. ferrihydrites ($Fe^{3+}{}_{10}O_{14}(OH)_2$)), which are typical for bog iron ores (Banning, 2008). Diffraction reflexes of amorphous minerals are only detectable through background noise in the unprocessed XRD-diffractograms (Appendix, Figs. A.4, A.6, A.11 and A.13), which leads to an underestimation of iron mineral contents compared to elemental iron contents from the *p*-ED-XRF analyses (Table 4).

In their elemental composition the bog iron ores from the study area show typical contents (cf. Section 1.1.1), which are dominated by iron (Fe_2O_3) and silicon (SiO_2) and supplemented by considerable manganese (MnO) and phosphorus (P_2O_5) contents (Graupner, 1982; Sperling, 2003). The existing very strong, negative linear correlation between iron and silicon, with a correlation coefficient of $R = -0.93$ (Fig. 4) in the samples from the study area represents a typical pattern for bog iron ores of different qualities. Thus this correlation is also observable in the results from the literature review (Table 1; Fig. 1A) with a correlation coefficient of $R = -0.82$ (Appendix, Fig. A.2). This pattern represents different stages in the bog iron ore formation process (Fig. 4). During this process the changing matrix-component ratio leads to a change of the iron-silicon ratio. The higher the iron contents are, the lower the relative silicon content and the further developed the bog iron ores from initial soft stages to hardened, compacted bog iron ore layers (Fig. 4). Especially the bog iron ores with lower iron contents, sampled at the study site of Młokicie (Table 4), are characterized by soft concretions representing a typical initial bog iron ore development stage (Kaczorek et al., 2004), whereas the samples from the study site of Rychnów represent a rather developed type of bog iron ore (Fig. 4).

Regarding the quality for iron smelting in the study area, the iron-hydroxide contents of between 1.6 and 64.9 mass% Fe_2O_3 (equivalent to 1.1 and 45.4 mass% Fe) of all collected initial and developed bog iron ore samples (Table 4) are situated in the lower midfield compared to the literature review from Poland, Germany and the Netherlands (Fig. 1A; Table 1): Only in Mazovia (Poland) the iron contents are lower than in the study area (Hensel, 1986). Also the applied 1- and 2-tailed *U* tests confirmed that the iron contents of the bog iron ores from the comparative studies tend to be higher. As bog iron ores often show increased manganese and phosphorus contents (Graupner, 1982; Sperling, 2003), the contents of these elements in the ores of the study area are typical with values between 0.1 and 5.7 mass% MnO and 0.5 and 6.9 mass% P_2O_5 (Table 4). Highest manganese contents are associated to the samples from Młokicie (riverbed), whereas highest phosphate contents occurred in the samples from Rychnów. The range of these variations is similar to values from comparative studies, which show manganese and phosphorus contents of between 0.1 and 13.5 mass% MnO and 0.4 and 8.4 mass% P_2O_5 (Table 1). According to Iles (2014), Heimann et al. (2001) and Graupner (1982) manganese overall has a positive effect on the smelting process (cf. Section 1.1.5), while the phosphorus content can – depending on the process temperatures – decrease the quality of the produced iron (cf. Section 1.1.5; Graupner, 1982; Bauermeister and Kronz, 2006; Sperling, 2003; Puttkammer, 2012).

The influence of element measurements exceeding the standard values on the PCA is regarded as comparatively negligible due to the clear linear correlation between the standard reference materials and the XRF-results. PC 1 from the PCA of bog iron ores represents with iron (Fe_2O_3) and silicon (SiO_2) the main quality measure of the ores in terms of their suitability for prehistoric iron smelting: the lower the PC 1 value, the higher the Fe_2O_3 and the lower the SiO_2 contents. A low PC 1 also represents high phosphorus contents (Fig. 5B). PC 2 particularly represents manganese (MnO) and barium (BaO) contents: the higher the PC 2 value, the higher the MnO and BaO contents (Fig. 5B). Thus, higher iron and manganese contents are represented in the PCA by a low PC 1 and a high PC 2 (Fig. 5A). These are according to Iles (2014), Heimann et al. (2001) and Graupner (1982) overall improving the favorability for iron smelting with a bloomery furnace. The point cloud in the PCA-scatterplot (Fig. 5A) shows eight clusters, each representing a set of samples from different sites, pointing to a spatial variability of the chemical composition of the ores.

Distinctly higher iron contents were measured in the samples from Rychnów and Pielgrzymowice in comparison to those from Młokicie, Pawłowice and Wilków (Table 4). While the highest iron contents

Please cite this article as: Thelemann, M., et al., Bog iron ore as a resource for prehistoric iron production in Central Europe — A case study of the Widawa catchment area in eastern ..., Catena (2016), http://dx.doi.org/10.1016/j.catena.2016.04.002

with values up to 64.9 mass% Fe_2O_3 (equivalent to 45.4 mass% Fe; Table 4) result from Rychnów, iron contents above the empirical boundary value for iron smelting with a bloomery furnace of 55–60 mass% Fe (equivalent to 79–86 mass% Fe_2O_3) (Pleiner, 2000), are not reached in the samples. Therefore the samples from Rychnów represent ores that are most suitable for iron smelting in the study area. Whether these ores are indeed suitable for a successful iron smelting with a bloomery furnace depends not only on the iron content but also on the metal-slag separation in regard to available fluxing agents (Puttkammer, 2012). Altogether 20 smelting experiments with bloomery furnaces by Thiele (2010) in Hungary utilizing ores with iron contents of up to 67 mass% Fe_2O_3 (equivalent to up to 47 mass% Fe) indicate that the quality of the ores from the Widawa floodplain would be sufficient to obtain an iron bloom. Subsequent experiments showed that this bloom was too breakable for forging (Thiele, 2010). However the experiences and knowledge of early blacksmiths might have allowed obtaining better results.

4.2. Iron slags

The distribution of the slag sites in the study area, taken from the extensive archaeological survey, shows that these sites are bound to the margins of the Widawa floodplain (Fig. 2), similar to the detected bog iron ore sites (Fig. 2). The grey color and magnetic properties of the sampled slags from the Rychnów, Pielgrzymowice and Kowalowice site (Table 5) are typical for iron slags (Schwab et al., 2006; Shotyk, 1988). The lack of TIC and TOC contents are also characteristic of slags because during the iron-smelting process with temperatures of above 1100 °C the humus components are combusted and the calcium carbonates ($CaCO_3$) are thermally decomposed to calcium-oxide (CaO) and volatile carbon-dioxide (CO_2) (Dean 1974; Wang and Thomson, 1995).

Mineralogically, in contrast to the local bog iron ores, the slags from the study area hardly contain any quartz (Table 5). The silicon as well as the iron in the slags is mostly bound in fayalite (Fe_2SiO_4), an iron-silicon mineral, which is typical for iron slags (Puttkammer, 2012). Fayalite is formed from quartz and iron minerals in bog iron ores during the smelting process at between 1100 and 1400 °C (Joosten et al., 1998; Pollard and Heron, 1996), according to Puttkammer (2012) especially above 1200 °C. Since most of the iron is transferred into fayalite, other iron minerals, such as goethite (α-FeO(OH)), hematite (Fe_2O_3), siderite ($FeCO_3$) and pyrite (FeS_2) often only occur in traces, while wüstite (FeO) and maghemite (γ-Fe_2O_3) – as is typical (Schöner et al., 2003; Schwab, 2004) – occur as major or often as minor components. The occurrence of magnetite (Fe_3O_4) – as a ferric iron oxide – in the slag is rather untypical for an efficient smelting process and either points to an incomplete reduction or a formation of magnetite with oxygen from additional air supply (Manasse and Mellini, 2002).

Regarding the elemental composition of the sampled slags, the iron-oxide contents lie between 48.7 and 72.0 mass% FeO (equivalent to 37.9 and 56.0 mass% Fe) (Table 5). As two slag samples (slag11-1 and slag22-1, Table 5) show iron contents below 16.2 mass% FeO these samples probably represent melted furnace lining or slags contaminated by dissolved furnace lining (Joosten et al., 1998) and are not to be regarded as bloomery slags. Compared to the sampled ores the iron contents in the local slags are relatively high, especially if it is taken into account that 10 to 20 mass% Fe of the prehistoric slags has already been reduced to iron bloom (Puttkammer, 2012; Sperling, 2003). This indicates that the utilized prehistoric ores originally showed much higher iron contents than the analyzed samples. The variance in the iron contents of the sampled slags is also noticeable in the negative correlation of iron-oxides and silicon-dioxides ($R = -0.86$; Fig. 6). This pattern in the iron-silicon ratio (Fig. 4) results from the quality of utilized bog iron ores as well as from the process conditions in the furnace (Joosten et al., 1998). The linearity in the correlation between iron-oxides and silicon-dioxide in slags is typical and can also be observed in a joint iron-silicon plot (Appendix, Fig. A.3) of the results of the samples from the literature review (Table 2) with a negative correlation coefficient of $R = -0.77$. Most analyzed bloomery slags – with an *RII* below 1.0 – represent samples with excess iron retained in the slag, which points to a lower reduction efficiency (Charlton et al., 2010). Compared to the calculated *RII* of the comparative studies from the literature review (Table 2) the reduction efficiency in the slags of the study area is relatively high with 39% of the analyzed slags showing an *RII* above 1.0 (Tables 2 and 5). Iron smelting with a bloomery furnace is generally characterized as being relatively inefficient (Sperling, 2003). An iron content of >50 mass% Fe (equivalent to 64 mass% FeO), as it was measured in most of the slags from the study area (Table 5), even indicates a "very inefficient reduction process" (Mihok, 2006; Heimann et al., 2001). Those iron quantities are most oftenly accompanied by a lower *RII* (Tables 2 and 5). Nevertheless the Fe contents in the slags of the study area are, apart from the mentioned outliers, of similar but lower magnitude than the results of the comparative studies (Fig. 1A; Table 2), also confirmed by the applied 1- and 2-tailed *U* tests. These lower contents can either indicate lower iron contents in the prehistoric ores used (Puttkammer, 2012) or a higher efficiency of the smelting process (Joosten et al., 1998).

Increased manganese and phosphorus contents are characteristic for iron slags produced from bog iron ores (Table 2; Gordon, 1996; Photos-Jones and Atkinson, 1998). This characteristic can be used to differentiate slags from bog iron ores and iron gangue minerals. With values of up to 8.6 mass% MnO the analyzed samples show particularly high manganese contents even for bog iron ores. The phosphorus contents – with up to 7.3 mass% P_2O_5 – are mostly lower than in comparative studies (Tables 2 and 5) but are still typical for iron slags produced from bog iron ores (Kaczorek et al., 2004; Sperling, 2003; Oberrascher, 1939).

Principal component 1 mainly represents the iron and silicon contents, which correlate with the reduction efficiency of the smelting processes or the quality of smelted ores: the higher PC 1, the higher the FeO and the lower the SiO_2 contents. Furthermore a high PC 1 value also represents low Al_2O_3, K_2O, TiO_2 and CaO contents. In contrast a high PC 2 mainly represents high BaO and P_2O_5 contents (Fig. 7B). Particularly for P_2O_5 with up to 7.3 mass% these results are again influenced by negligible inaccuracies with increasing element contents since the used reference material only reached 3.8 mass% (Table 5). The PC-plot of PC 1 against PC 2 of the sampled iron slags (Fig. 7A) shows a wide overlapping scattering of the slag samples from Pielgrzymowice and Kowalowice, while the slags from Rychnów show a relatively narrow distribution. These differences in the point patterns, which represent a wider variability in the elemental composition in the slags from Pielgrzymowice and Kowalowice than from Rychnów, indicate more distinctive differences in (i) the elemental composition of utilized ores, e.g. their phosphorus and manganese contents (Joosten et al., 1998; Graupner, 1982; Schwab, 2004) and (ii) contaminations with fuel ash, furnace lining and additional fluxing agents (Joosten et al., 1998; Koschke, 2002; Sperling, 2003) as well as in the process conditions, such as (iii) the process temperatures (Puttkammer, 2012; Joosten et al., 1998), (iv) the duration, efficiency and homogeneity of the smelting process (Garner, 2011; Schwab et al., 2006; Joosten et al., 1998) and/or (v) the utilized furnace type (Schöner et al., 2003; Degryse et al., 2009). In contrast to the relatively consistent elemental composition of the slags from Rychnów there seems to be no typical elemental composition for the iron slags from Pielgrzymowice and Kowalowice (Fig. 7A).

5. Conclusions

In the study area bog iron ores of varying quality are relatively widely distributed. The detected ores are situated at the margins of the Widawa floodplain (Rychnów and Młokicie) or by its tributaries (Pawłowice) at wetter topographic positions between Holocene fluvial and Saalian glacial deposits. The ores are characterized by a typical,

Please cite this article as: Thelemann, M., et al., Bog iron ore as a resource for prehistoric iron production in Central Europe — A case study of the Widawa catchment area in eastern ..., Catena (2016), http://dx.doi.org/10.1016/j.catena.2016.04.002

goethite-dominated mineralogical composition and a variety of different iron-silicon ratios, which represent different bog iron ore formation stages. With increasing iron and decreasing silicon contents the suitability of the ores for iron smelting with a bloomery furnace increases. The analyzed ores show significantly lower iron contents than those from studies in Poland, Germany and the Netherlands. Ores with iron contents of up to 64.9 mass% Fe_2O_3 originate from the study site of Rychnów. These ores show sufficient iron contents to produce an iron bloom with a bloomery furnace. The elemental variability of ores was investigated by conducting a principal component analysis, indicating a specific elemental ore composition at each sampling site.

The sampled prehistoric iron slags are characterized by a typical, fayalite-dominated mineralogical composition pointing to process temperatures above 1200 °C. Considerable manganese and phosphorus contents in the slags verify that bog iron ores and not (imported) ores from iron gangue minerals were used for smelting attempts. Compared to the sampled ores of the study area the iron contents in the local slags are relatively high, which indicates that the prehistoric ores utilized originally showed higher iron contents than the presently located ores. A principal component analysis of the major oxide concentrations in iron slags shows a higher variability in the elemental compositions of slags from Pielgrzymowice and Kowalowice, which indicates the utilization of ores of different quality and/or inhomogeneous smelting conditions in the bloomery furnaces. In contrast, a lower variability in the elemental composition of slags from Rychnów was revealed, suggesting more homogeneous ore compositions and smelting conditions. All in all the principal component analysis is regarded as a useful tool to investigate patterns in the elemental composition of iron slags and bog iron ores of different sub-sites of a study region.

In summary, several indicators suggest favorable conditions for prehistoric iron production in the study area: (i) There is a large number of known prehistoric slag sites in the study area, which contrasts to the few in-situ bog iron ore sites presently in existence, (ii) the iron contents in the local analyzed slags are comparable to other centers of early iron production, especially to the close-by study areas of Tarchalice and Milanówek (Poland), (iii) the iron contents in the prehistoric slags are relatively high compared to the bog iron ores detectable nowadays, and (iv) despite the negative effects of deforestation, modern agriculture and melioration measures, bog iron ores probably suitable for iron production were even today detected in the study area. However, in the vicinities of slag sites, such as Pielgrzymowice and Lubska, recent in-situ ore deposits were not detected. The number of sampled sites and their density are too low in terms of identifying areas of higher favorability for the formation of bog iron ores within the study area. Anyhow, it can be stated that samples from different study sites show significantly different qualities of bog iron ores, with higher qualities at the study site of Rychnów and lower qualities at Młokicie, Pawłowice and Wilków.

The identified discrepancy in the iron contents of current bog iron ore deposits compared to prehistoric ores is ascribed to landscape changes induced by deforestation, intensified land-use practices and bog iron ore exploitation in the study area during the last millennia, as well as to a dryer and cooler climate compared to the main bog iron ore formation phase during the Atlantic. Therefore the present conditions do not reflect the resource situation in prehistoric times, when bog iron ores of higher quality could be exploited. Nevertheless our study has demonstrated that bog iron ores of varying quality, comparable to those found in comparative studies, are situated along the Widawa floodplain and that iron slags similar to those of other centers of early iron smelting were identified at the numerous prehistoric iron slag sites in the study area.

Acknowledgements

This study was supported by the Deutsche Forschungsgemeinschaft (DFG) within the Cluster of Excellence TOPOI EXC 264 (The Formation and Transformation of Space and Knowledge in Ancient Civilizations) and the collaboration of Topoi Research Group A-5 "Iron as a Raw Material". First of all we thank the reviewers for their very valuable remarks and advices, which substantially helped to improve the paper. We thank our cooperation partners from the Archaeological Institute of the University of Wrocław, Prof. Dr. Artur Błażejewski, and the Museum of Archaeology Wrocław, Dr. Paweł Madera, as fieldwork was only possible with their help and support. Additionally we would also like to thank Dipl.-Geogr. Johanna Seidel and the students of the field excursions 2013 and 2014 from the Institute of Geographical Sciences and the Institute of Prehistoric Archaeology of the Freie Universität Berlin. We are grateful to Frank Kutz (Institute of Geographical Sciences, Freie Universität Berlin), who supported the *p*-ED-XRF and XRD analyses. We would like to address our thanks to Dr. Martina Renzi, for providing slag samples from Spain for calibration and to the Department of Cultural Heritage Opole, Poland, for their datasets of prehistoric iron slag sites.

Appendix A. Supplementary data

Supplementary data associated with this article can be found, in the online version, at doi: http://dx.doi.org/10.1016/j.catena.2016.04.002. These data include the Google map of the most important areas described in this article.

References

Arocena, J., De Geyter, G., Landuydt, C., Stoops, G., 1990. A study on the distribution and extraction of iron (and manganese) in soil thin sections. Dev. Soil Sci. 19, 621–626.
Archeologiczne Zdjęcie Polski, since 1978. Unpublished archaeological catalogue. Department of Cultural Heritage Opole, Poland.
Banning, A., 2008. Bog iron ores and their potential role in arsenic dynamics: an overview and a "Paleo Example". Eng. Life Sci. 8, 641–649.
Banning, A., Rüde, T., Dölling, B., 2013. Crossing redox boundaries — aquifer redox history and effects on iron mineralogy and arsenic availability. J. Hazard. Mater. 262, 905–914.
Bartczak, E., 1997. Geological detailed map, 1: 50 000. Map sheet 0766. Polish Geological Institute, National Research Institute.
Bauermeister, J., Kronz, A., 2006. Phosphorreiche Erze: Ein Problem für die frühe Eisenverhüttung? - Kaiserzeitliche Eisenverhüttung im Kreis Leer. Archäom. und Denkmalpfl. 55–57.
Bebermeier, W., Brumlich, M., Cordani, V., de Vincenzo, S., Eilbracht, H., Hofmann, A., Klinger, J., Knitter, D., Lehnhardt, E., Meyer, M., Schmid, S.G., Schütt, B., Thelemann, M., Ullrich, B., Wemhoff, M. 2016. eTopoi, J. for Anc. Special Volume. Berlin (accepted) (2016).
Blakelock, E., Martinón-Torres, M., Veldhuijzen, H., Young, T., 2009. Slag inclusions in iron objects and the quest for provenance: an experiment and a case study. J. Archaeol. Sci. 36, 1745–1757.
Brumlich, M., Meyer, M., Lychatz, B., 2012. Archäologische und archäometallurgische Untersuchungen zur latènezeitlichen Eisenverhüttung im nördlichen Mitteleuropa. Praehist. Z. 87, 433–473.
Buchwald, F., 2005. Iron and Steel in Ancient Times. The Royal Dan. Academy of Sci. and Letters, Viborg.
Buurman, P., Jongmans, A., 2005. Podzolisation and soil organic matter dynamics. Geoderma 125, 71–83.
Charlton, M., Crew, P., Rehren, T., Shennan, S., 2010. Explaining the evolution of ironmaking recipes – an example from northwest Wales. J. Anthropol. Archaeol. 29, 352–367.
Charlton, M., Blakelock, E., Martinón-Torres, M., Young, T., 2012. Investigating the production provenance of iron artifacts with multivariate methods. J. Archaeol. Sci. 39, 2280–2293.
Cincio, Z., 1997. Geological detailed map, 1: 50 000. Map sheet 0767. Polish Geological Institute, National Research Institute.
Climate-Data.org., 1982–2012. AmbiWeb GmbH. http://en.climate-data.org/location/10308/ Last access 01.12.2014.
CODGiK, 2013. Centralny Ośrodek Dokumentacji Geodezyjnej I Kartograficznej. Central Documentation Center for Geodesy and Cartography, Poland.
Conrads, N., 1994. Silesiographia oder Landschaftsbeschreibung. Deutsche Geschichte im Osten Europas. Wolf Jobst Siedler Verlag GmbH, Berlin, pp. 13–20.
Correns, C., 1969. Introduction to Mineralogy, Crystallography, and Petrology. second ed. Springer-Verlag, Berlin Heidelberg New York.
Crew, P., Charlton, M., Dillmann, P., Fluzin, P., Salter, C., Truffaut, E., 2011. Cast iron from a bloomery furnace. In: Hošek, J., Cleere, H., Mihok, L. (Eds.), The Archaeometallurgy of Iron - Recent Developments in Archaeological and Scientific Research, Prague, pp. 237–262.
Dąbrowska, T., 2003. Przeworsk-Kultur. Reallexikon der Germanischen Altertumskunde 23. Walter de Gruyter, Berlin, pp. 540–567.
Dean, W., 1974. Determination of carbonate and organic matter in calcareous sediments and sedimentary rocks by loss on ignition: comparison with other methods. J. Sediment. Petrol. 44, 242–248.

ARTICLE IN PRESS

Degryse, P., Schneider, J., Muchez, P., 2009. Combined Pb–Sr isotopic analysis in provenancing late Roman iron raw materials in the territory of Sagalassos (SW Turkey). Archaeol. Anthropol. Sci. 155–159 (Springer-Verlag).
De Vries, J., Vrebos, B., 2002. Quantification of infinitely thick specimens by XRF analysis. In: Van Grieken, R., Markowicz, A. (Eds.), Handbook of X-Ray Spectrometry, Second revised and expanded ed. Marcel Dekker, New York, Basel, pp. 341–406.
De Rijk, Patrice, 2003. De scoriis – Eisenverhüttung und Eisenverarbeitung im nordwestlichen Elbe-Weser-Raum. PhD Thesis. Instituut voor Cultuur en Geschiedenis. University of Amsterdam.
Domanski, G., 1972. Stanowisko Hutnicze I Osady Z Tarchalic, Pow. Wołów, Stan. 1. Sprawozdania Archeologiczne, t. XXIV pp. 391–438.
Evenstad, O., 1801. Abhandlung Von den Sumpf- und Morast-Eisensteinen in Norwegen und von der Methode solche in so genannten Bauer- oder Blaseöfen in Eisen und Stahl zu verwandeln. Dieterichische Buchhandlung, Göttingen.
Fahrmeir, L., Hamerle, A., Tutz, G., 1996. Multivariate statistische Verfahren 2. Walter de Gruyter, Berlin, New York.
Gall, B., Schmidt, R., Bauriegel, A., 2003. Gley mit Raseneisenerde. Steckbriefe Brandenburger Böden. Ministerium für Landwirtschaft, Umweltschutz und Raumordnung Landes Brandenburg (Editor), Referat Bodenschutz Potsdam pp. 1–4.
Garner, J., 2011. Der latènezeitliche Verhüttungsplatz in Siegen-Niederschelden "Wartestraße". Metalla (Bochum) 1–148.
Godłowski, K., 1985. Przemiany kulturowe i osadnicze w południowej i środkowej Polsce w młodszym okresie przedrzymskim i w okresie rzymskim, in: Prace Komisji Archeologicznej / Polska Akad. Nauk, Oddział w Krakowie 23. Ossolińskich, Wrocław, Zakład Narodowy im.
Gordon, R., 1996. American Iron – 1607 and 1900. Johns Hopkins University Press, Baltimore and London.
Graupner, A., 1982. Raseneisenstein in Niedersachsen. Entstehung, Vorkommen, Zusammensetzung und Verwendung. Forschungen zur niedersächsischen Landeskunde 118. Kommissionsverlag Göttinger Tageblatt GmbH & Co. KG., Göttingen.
Hartmann, K., Wünnemann, B., 2007. Hydrological Changes and Holocene Climate Variations in NW China, Inferred From Lake Sediments of Juyanze Palaeolake by Factor Analyses. Quat, Internatl.
Heimann, R., Kreher, U., Spazier, I., Wetzel, G., 2001. Mineralogical and chemical investigations of bloomery slags from prehistoric (8th century BC to 4th century AD) iron production sites in upper and lower Lusatia. Germany. Archaeom. 43, 227–252.
Hensel, Z., 1986. Z Badan Nad Technologia Otrzymywania Zelaza Na Terenie Mazowieckiego Osrodka Metalurgicznego, in: Archeologia Polski. TOM XXXI. Zeszyt 1, 31–90.
Huisman, D., Vermeulen, F., Baker, J., Veldkamp, A., Kroonenberg, S., Klaver, G., 1997. A geological interpretation of heavy metal concentrations in soils and sediments in the southern Netherlands. J. Geochem. Explor. 59, 163–174.
Iles, L., 2014. The exploitation of manganese-rich 'ore' to smelt iron in Mwenge, western Uganda, from the mid second millennium AD. J. of Arch. Sc. 49, 423–441.
Jenkins, R., 1999. X-Ray Fluorescence Spectrometry. second ed. John Wiley & Sons, New York, pp. 341–405.
Joosten, I., Jansen, B., Kars, H., 1998. Geochemistry and the past: estimation of the output of a Germanic iron production site in the Netherlands. J. Geochem. Explor. 62, 129–137.
Kaczorek, D., Sommer, M., 2003. Micromorphology, chemistry, and mineralogy of bog iron ores from Poland. Catena 54, 393–402.
Kaczorek, D., Sommer, M., Andruschkewitsch, I., Oktaba, L., Czerwinski, Z., Stahr, K., 2004. A comparative micromorphological and chemical study of "Raseneisenstein" (bog iron ore) and "Ortstein". Geoderma 121, 83–94.
Kaczorek, D., Brümmer, G., Sommer, M., 2005. Content and binding forms of heavy metals. Aluminium and phosphorus in bog iron ores from Poland. J. Environ. Qual. 38, 1109–1119.
Koschke, W., 2002. Raseneisenerz und Eisenhüttenindustrie in der nördlichen Oberlausitz, 18. Freundeskreis Stadt- und Parkmuseum, Bad Muskau.
Krempler, M., Siedel, H., Schlütter, F., Wendler, E., 2004. Mineralogisch-petrographische Beschreibung, Materialklassifizierung und –kartierung, in: Brandenburgisches Landesamt für Denkmalpflege und Archäologisches Landesmuseum, Raseneisenstein - Untersuchung und Konservierung. Arbeitshefte des Brandenburgischen Landesamtes für Denkmalpflege und Archäologisches Landesmuseum 11, 1–40.
Küster, H., 1999. Geschichte der Landschaft in Mitteleuropa. Von der Eiszeit bis zur Gegenwart. Beck Verlag, München.
Kuttler, W., 2009. Klimatologie. Verlag Ferdinand Schöningh, Paderborn.
KZGW, 2015. Polish National Department for Water Management http://mapa.kzgw.gov.pl/ last access 10.11.2015.
Landuydt, C., 1990. Micromorphology of iron minerals from bog ores of the Belgian Campine area. Basic and Appl. Sci. 19, 289–294.
Last, W., 2001. Mineralogical analysis of lake sediments. In: Last, W., Smol, J. (Eds.), Tracking Environmental Change Using Lake Sediments Volume 2: Physical and Geochemical Methods. Kluwer Academic Publishers, Dordrecht.
Leb, M., 1983. Raseneisenerze in der Oberlausitz - Ein Beitrag zur Geschichte der Raseneisenerzverarbeitung und Geologie der Erzvorkommen. Sächsische Heimatblätter 29, 127–132.
Liedtke, H., 1981. Die Nordischen Vereisungen in Mitteleuropa. Forschungen zur Deutschen Landeskunde. Volume 204, second extended ed. Zentralausschuss der Deutschen Landeskunde, Trier.
Lindbo, D., Stolt, M., Vepraskas, M., 2010. Redoximorphic features. In: Stoops, G., Marcelino, V., Mees, F. (Eds.), Interpretation of Micromorphological Features of Soils and Regoliths, pp. 129–147.
Madera, P., 2002. Ślady starożytnego hutnictwa żelaza na Śląsku w ujęciu chronologiczno-przestrzennym. In: Orzechowski, S. (Ed.), Ślady starożytnego hutnictwa żelaza na Śląsku w ujęciu chronologiczno-przestrzennym. Śląsk, Świętokrzyskie Stowarzyszenie Dziedzictwa Przemysłowego. Kielce, pp. 61–70.
Manasse, A., Mellini, M., 2002. Chemical and textural characterisation of medieval slags from the Massa Marittima smelting sites (Tuscany, Italy). J. Cult. Herit. 3, 187–198.
Mihok, L., 2006. Beginnings of iron smelting in the Central Carpathians region. Metalurgija – J. of Metall. 12, 173–184.
Oberrascher, E., 1939. Die Raseneisenerze Pommerns. Geologisch-Paläontologisches Institut der Ernst-Moritz-Arndt-Universität Greifswald, Greifwald.
Orzechowski, S., 2007. The Region of Iron: The Przeworsk Culture Iron Producing Centre in Barbaricum. In: Crew, P., Crew, S. (Eds.), Early Ironworking in Europe II, Archaeology, Technology and Experiment. Second International Conference Plas Tan Y Bwlch. Wales, pp. 27–28.
Orzechowski, S., 2011. Canal-pit and its role in the bloomery process: the example of the Przeworsk culture furnaces in the Polish territories. In: Hošek, J., Cleere, H., Mihok, L. (Eds.), The Archaeometallurgy of Iron - Recent Developments in Archaeological and Scientific Research, Prague, pp. 41–54.
Pawlak, W., 1997. Atlas of Lower and Opole Silesia. Map Sheet 28. University of Wrocław and Academy of Science, Poland – Department Wrocław.
Paynter, S., 2006. Regional variations in bloomery smelting slag of the iron age and Romano-British periods. Archaeom. 48, 271–292.
Pelzer, F., 1991. Eine geographische Landeskunde, 36. Wissenschaftliche Buchgesellschaft, Darmstadt.
Photos-Jones, E., Atkinson, J., 1998. Iron-working in medieval Perth — a case of town and country? Proc. Soc. Antiqu. Scotl. 128, 887–904.
Piaskowski, J., 1976. Classification of the Structures of Slag Inclusions in Early Objects Made of Bloomery Iron. Archaeologia Polona XVII, pp. 139–149.
Pleiner, R., 2000. Iron in Archaeology. The European Bloomery Smelters. Archeologický ústav AV CR, Prague.
Pollard, M., Heron, C., 1996. Archaeological Chemistry. The Royal Society of Chemistry - RSC Paperbacks, Cambridge.
Postawa, A., Hayes, C., 2013. Best Practice Guide on the Control of Iron and Manganese in Water Supply. IWA Publishing, London.
Puttkammer, T., 2012. Auf den Spuren der Germanen. Begleitband zur Wanderausstellung. Museum der Westlausitz, Kamenz.
Ramsey, M., Potts, P., Webb, P., Watkins, P., Watson, J., Coles, B., 1995. An objective assessment of analytical method precision: comparison of ICP-AES and XRF for the analysis of silicate rocks. Chem. Geol. 124, 1–19.
Ratajczak, T., Rzepa, G., 2011. Lokalne Kopaliny Mineralne A Możliwości Ich Wykorzystania W Ochronie Środowiska (Na Przykładzie Mazurskich Rud Darniowych) Inżynieria Ekologiczna 27, 161–169.
Rinne, H., 2008. Taschenbuch der Statistik,. Ffourth completely revised and extended ed. Wirtschaftlicher Verlag Harri Deutsch, Frankfurt/Main.
Rössner, T., 1998. Die mitteleuropäische West-Ost-Achse Sachsen-Schlesien-Galizien. Institut für Länderkunde, Leipzig.
Rzepa, G., Bajda, T., Ratajczak, T., 2009. Utilization of bog iron ores as sorbents of heavy metals. J. Hazard. Mater. 162, 1007–1013.
Salesch, M., 1996. Raseneisenstein im Elbe-Elster-Kreis. Natur und Landschaft in der Niederlausitz 17, 43–53.
Schöner, R., Scholz, H., Krumm, H., 2003. Die mittelalterliche Eisengewinnung im Füssener Land (Ostallgäu und Außerfern): Neue Ergebnisse zum Abbau und zur Verhüttung der Eisenerze aus dem Wettersteinkalk. Archiv für Lagerstättenforschung der Geologischen Bundesanstalt 24, 193–218.
Schütt, B., 2004. Zum holozänen Klimawandel der zentralen Iberischen Halbinsel. In: Bremer, H., Heine, K., Lauer, W., Hagedorn, H. (Eds.), Relief Boden Paläoklima 20. Gebrüder Borntraeger, Berlin, Stuttgart.
Schwab, R., 2004. Technologie und Herkunft eiserner Werkzeuge und Waffen aus dem spätkeltischen Oppidum von Manching. Dissertation, TU Bergakademie Freiberg.
Schwab, R., Heger, D., Höppner, B., Pernicka, E., 2006. The provenance of iron artefacts from Manching: a multi-technique approach. Archaeom. 48, 433–452.
Shotyk, W., 1988. Review of the inorganic geochemistry of peats and peatland waters. Earth-Sci. Rev. 25, 95–197.
Sitschick, H., Ludwig, F., Wetzel, E., Luckert, J., Höding, T., 2005. Raseneisenerz – auch in Brandenburg ein mineralischer Rohstoff mit bedeutender wirtschaftlicher Vergangenheit. Brandenburgische Geowissenschaftliche Beiträge 12, 119–128.
Sperling, D., 2003. Rohstoffgewinnung und Altbergbau im Förderraum Calau. Beiträge zur Geschichte des Bergbaus in der Niederlausitz 3. Niederlausitz e.V. Cottbus, Förderverein Kulturlandschaft.
Thelemann, M., Lehnhardt, E., Bebermeier, W., Meyer, M., 2016. Iron, human and landscape – insights from a micro-region in the Widawa Catchment Area, Silesia. Exzellenzcluster 264 Topoi. Issue bridging the gap – integrated approaches in landscape archaeology. eTopoi, J. for Anc. Stud., Special Volume 4. Berlin (in press) (2016).
Thiele, A., 2010. Smelting experiments in the early medieval fajszi-type bloomery and the metallurgy of iron bloom. Mech. Eng. 54/2, 99–104.
TK25, 1886–1938. Topographic map 1: 25 000, plane-table sheets 4871 (Bernstadt, 1899), 4872 (Schmograu, 1886), 4971 (Lampersdorf, 1912) and 4972 (Namslau, 1938). Preußische Landesaufnahme.
USGS, 2000. U.S. Geological Survey. SRTM-data set 1 Arc-Second Global. http://earthexplorer.usgs.gov/ Last access 10.10.2015.
Veldhuijzen, H.A., Rehren, T., 2007. Slags and the city: early iron production at Tell Hammeh, Jordan, and Tel Beth-Shemesh, Israel. In: La Niece, S., Hook, D., Craddock, P. (Eds.), Metals and Mines: Studies in Archaeometallurgy. Archetype/British Museum, London, pp. 189–201.
Wang, Y., Thomson, W., 1995. The effect of sample preparation on the thermal decomposition of $CaCO_3$. Thermochim. Acta 255, 383–390.
Wiatkowski, M., Rosik-Dulewska, C., Tyminski, T., 2010. Analysis of water management of the Michalice reservoir in relation to its functions. Society of Ecological Chemistry and

Please cite this article as: Thelemann, M., et al., Bog iron ore as a resource for prehistoric iron production in Central Europe — A case study of the Widawa catchment area in eastern ..., Catena (2016), http://dx.doi.org/10.1016/j.catena.2016.04.002

ARTICLE IN PRESS

Engineering, Ministry of Sci. and Higher Education, Warszawa. Opole. Ecol. Chem. Eng. 17 (11), 1505–1515.
Woźniak, Z., 1978. A survey of the investigations of the Bronze and Iron Age sites in Poland in 1977. Sprawozdania Archeologiczne 30, 263–269.
Wünsche, D., 2007. Genese, Nutzung und Verbreitung von Mooren. GRIN Verlag GmbH, München.
Yalçin, Ü., 2000. Zur Technologie der frühen Eisenverhüttung. Arbeits- und Forschungsberichte zur Sächsischen Bodendenkmalpflege 42, 307–316.
Zhang, Y., Zhao, F., Wang, Y., 2011. Effects of influencing factors on distribution behaviors of vanadium between hot metal and FeO-SiO2-MnO (−TiO2) slag system. Steel Res. Int. 82, 940–950.
Zwahr, H., Granitzki, K., Schomburg, J., Zander, H.-J., 2000. Quartäres Raseneisenerz in Mecklenburg-Vorpommern - Genese Stoffbestand, Vorkommen und Nutzung. Brandenburgische Geowissenschaftliche Beiträge 7, 83–91.

Please cite this article as: Thelemann, M., et al., Bog iron ore as a resource for prehistoric iron production in Central Europe — A case study of the Widawa catchment area in eastern ..., Catena (2016), http://dx.doi.org/10.1016/j.catena.2016.04.002

View publication stats